

DOE/FE/60177-2392
(DE87013750)
Distribution Category UC-109

**PHYSICAL AND NUMERICAL MODELING
RESULTS FOR CONTROLLING GROUNDWATER
CONTAMINANTS FOLLOWING SHUTDOWN OF
UNDERGROUND COAL GASIFICATION PROCESSES**

By

**J. E. Boysen
C. G. Mones
R. R. Glaser
S. Sullivan**

March 1987

**Work Performed Under Cooperative Agreement
DE-FC21-83FE60177**

For

**U.S. Department of Energy
Office of Fossil Energy
Morgantown Energy Technology Center
Laramie Project Office
Laramie, Wyoming**

By

**Western Research Institute
Laramie, Wyoming**

TABLE OF CONTENTS

	<u>Page</u>
LIST OF TABLES.....	iii
LIST OF FIGURES.....	iv
SUMMARY	v
INTRODUCTION.....	1
TECHNICAL DISCUSSION.....	2
General.....	2
Numerical Simulation.....	4
Model Formulation.....	4
Model Equations.....	4
Numerical Solution.....	7
Model Verification.....	7
Physical Simulation.....	8
Reactor Design.....	8
Reactor Material Selection.....	8
Reactor Controls and Instrumentation.....	10
Experimental Procedure.....	10
Sampling and Analyses.....	12
RESULTS AND DISCUSSION.....	12
Shakedown.....	12
Initial Series of Physical Simulations.....	13
Simulation Results.....	14
Pyrolysis Zone Penetration.....	14
Contaminant Production and Migration.....	17
CONCLUSIONS.....	22
Experimental Conclusions.....	22
Recommendations for UCG Field Testing.....	23
Current Research.....	23
ACKNOWLEDGMENTS.....	24
DISCLAIMER.....	24
REFERENCES.....	25
APPENDIX A: NOMENCLATURE AND VALUES FOR PARAMETERS USED IN THE NUMERICAL MODEL.....	26
APPENDIX B: EXPERIMENTAL CHEMICAL ANALYSES.....	30
APPENDIX C: EXPERIMENTAL TEMPERATURE DATA.....	34
APPENDIX D: EXPERIMENTAL DATA FOR PHENOLS.....	40
APPENDIX E: EXPERIMENTAL DATA FOR OTHER EXPERIMENTS.....	46

LIST OF TABLES

<u>Table</u>		<u>Page</u>
1.	Postburn UCG Coal Pyrolysis Physical Simulation Experimental Conditions and Pyrolysis Zone Penetration.....	13
2.	Phenol Concentrations of the Liquids Produced During the Physical Simulations.....	21
3.	Phenol Distribution Between the Coal and Produced Liquids...	21
4.	Other Contaminant Species Generated During Coal Pyrolysis...	22
B-1.	Full Suite of Analyses for Produced Liquids and Injected Water.....	32
D-1.	Phenol Concentrations of Coal Samples.....	41
E-1.	Total Organic Carbon (TOC) Concentrations.....	47
E-2.	Sulfate Concentrations.....	48
E-3.	Ammonia (NH ₃ -N) Concentrations.....	49
E-4.	Boron (B) Concentrations.....	50
E-5.	Fluoride (F) Concentrations.....	51
E-6.	Barium (Ba) Concentrations.....	52
E-7.	Arsenic (As) Concentrations.....	53
E-8.	Selenium (Se) Concentrations.....	54
E-9.	Lead (Pb) Concentrations.....	55
E-10.	Mass of Contaminant Species in the Produced Liquids.....	56
E-11.	Other Contaminant Species Generated During Coal Pyrolysis.....	57

LIST OF FIGURES

<u>Figure</u>		<u>Page</u>
1.	Simulation of UCG Postburn Pyrolysis.....	3
2.	Contaminant Control Reactor.....	9
3.	Contaminant Control Reactor Piping and Instrument Diagram... 11	
4.	Temperature Profiles of Coal Core for Experiment No. 7.....	15
5.	Pyrolysis Zone Penetration Versus Rate of Water Injection Through Coal With Cavity Vented.....	16
6.	Pyrolysis Zone Penetration Versus Rate of Water Injection Into Cavity.....	18
7.	Maximum Temperature and Phenol Concentration Versus Position for Experiment No. 3.....	19
8.	Maximum Temperature and Phenol Concentration Versus Position for Experiment No. 5.....	20
C-1.	Temperature Profiles of Coal Core for Experiment No. 3.....	35
C-2.	Temperature Profiles of Coal Core for Experiment No. 4.....	36
C-3.	Temperature Profiles of Coal Core for Experiment No. 5.....	37
C-4.	Temperature Profiles of Coal Core for Experiment No. 6.....	38
C-5.	Temperature Profiles of Coal Core for Experiment No. 8.....	39
D-1.	Maximum Temperature and Phenol Concentration Versus Position for Experiment No. 4.....	42
D-2.	Maximum Temperature and Phenol Concentration Versus Position for Experiment No. 6.....	43
D-3.	Maximum Temperature and Phenol Concentration Versus Position for Experiment No. 7.....	44
D-4.	Maximum Temperature and Phenol Concentration Versus Position for Experiment No. 8.....	45

SUMMARY

Previous field tests have demonstrated the technical feasibility and confirmed the commercial potential of underground coal gasification (UCG). However, groundwater contamination has resulted from some of these tests, and concern over groundwater contamination may hamper commercialization. When UCG recovery operations are terminated, energy remains stored as heat in the adjacent masses of rock and coal ash, and this energy is transferred into the coal seam. Coal continues to pyrolyze as a result of the transferred energy; the products of this coal pyrolysis are a source of groundwater contamination resulting from UCG.

A laboratory simulator was developed, and six simulations of UCG postburn coal pyrolysis have been completed. The simulations show that the products of coal pyrolysis are the source of most contaminants associated with UCG operations. Injection of water directly into the UCG cavity can limit postburn coal pyrolysis and reduce the production of contaminants by cooling the masses of rubble and coal ash in the cavity. However, if the injected water forms channels as it flows through the cavity, the cooling effect is localized and the benefit of the water injection in limiting postburn coal pyrolysis is greatly reduced. Water flow through the coal towards the cavity also limits postburn pyrolysis and subsequent contaminant generation; however, steam produced in the heated portions of the coal limits the rate of water flow.

Simulation results indicate that UCG field tests should be operated so that the flow of pyrolysis liquids and gases into the formation is prevented and that the natural influx of water into the cavity is allowed. This can be accomplished by minimizing gas leakage to the formation during gasification, venting the cavity after the gasification process is complete, and maintaining low postburn cavity pressures.

INTRODUCTION

A research program has been initiated to investigate the production and control of groundwater contaminants following shutdown of in situ energy recovery processes. The major uncertainties of these processes are related to environmental problems. The key environmental problem is the potential pollution of groundwater and the associated uncertainty regarding the cost of groundwater restoration.

The general objectives of this research are to:

1. develop a laboratory simulator for investigating contaminant production occurring after in situ thermal recovery processing is complete,
2. shakedown the simulator and develop operational procedures for simulation,
3. develop a numerical simulation for thermal behavior of the resource to aid in predicting field behavior, and
4. provide data to determine the source of contaminant generation.

While this research program has potential applications to in situ thermal processes for recovery of energy from coal, oil shale, tar sands, and oil, the research focuses initially on contaminant production and migration occurring after shutdown of underground coal gasification (UCG) operations.

UCG is a process for producing energy from coal without mining. UCG field experiments in subbituminous coal deposits have successfully demonstrated the technical feasibility of producing gas from in place coal (Covell et al. 1980; Hill et al. 1980; Ahner 1982). Economic data indicate commercial potential for the process, but the uncertainty of the environmental impact resulting from the process may hamper commercial development. The contamination of groundwater resulting from UCG is a key environmental concern (Cooke and Oliver 1985).

The source of groundwater contamination resulting from UCG is believed to be the products of coal pyrolysis. During UCG operations, these products are produced at ground surface and do not contaminate groundwater unless the products escape into the underground formation. After UCG operations are finished, coal pyrolysis continues and these products become potential groundwater contaminants.

The apparent mechanism for postburn groundwater contamination is as follows: When oxidant injection is stopped, combustion ceases; but large masses of coal ash and rock remain at high temperatures. The energy in these masses slowly dissipates with time by heat conduction to adjacent portions of the resource. This conductive heating pyrolyzes part of the adjacent coal resource, and the resulting liquids and gases can introduce contaminants into the groundwater. Gradually, the high temperatures in the formation decrease and coal pyrolysis stops. However, the pyrolysis products remain in the coal seam, and soluble

contaminants are transported from the cavity by the natural flow of groundwater (Glaser and Owen 1986). The production of pyrolysis products following shutdown of UCG recovery operations and the resulting groundwater contamination have not been previously investigated. The results of this research enhance the understanding of how the UCG mechanism behaves and break new ground by testing hypotheses developed to gasify coal underground in an environmentally acceptable manner.

The initial series of eight experiments is complete. Two of these experiments were required to shakedown the laboratory equipment and develop operating procedures for the physical simulations. The other six experiments simulated (1) the reduction and removal of contaminants and (2) the relationship between contaminants and water influx rates and sources.

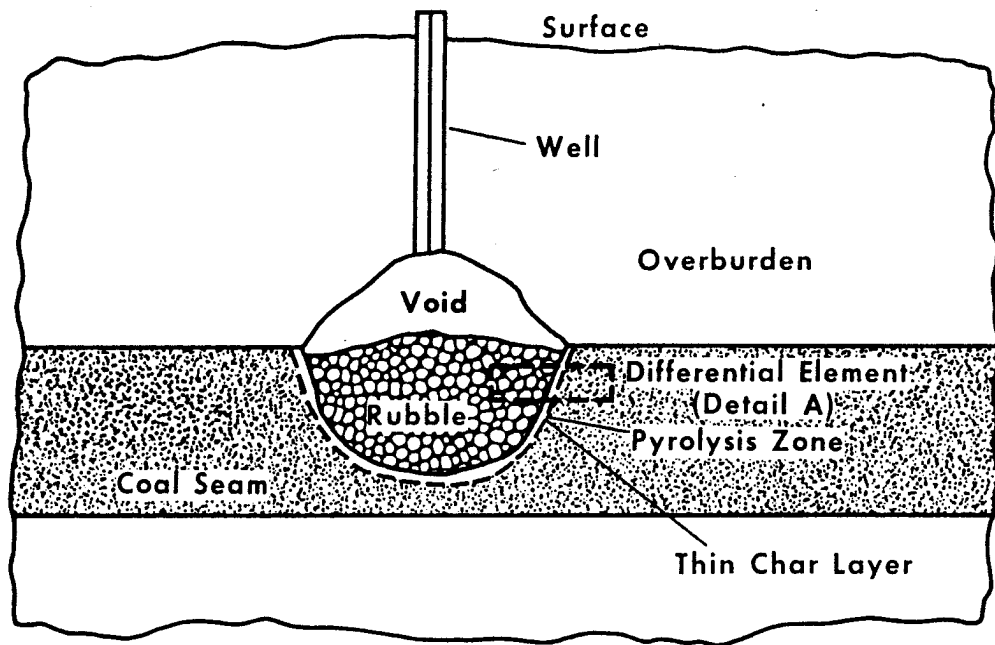
TECHNICAL DISCUSSION

General

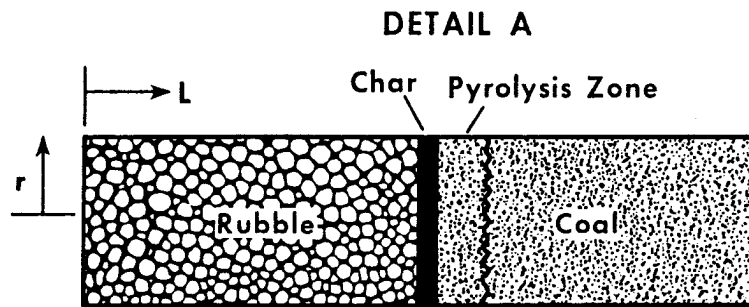
Data from the excavation of a UCG test (Oliver 1986) were used to produce a simplified schematic of postburn in situ conditions. The schematic illustrates a coal seam with an area that has been gasified and partially filled with hot ash and rubble from thermally affected coal and collapsed overburden (Figure 1). After injection shutdown, both the rubble and the thin char layer surrounding the cavity are at high temperatures. These postburn conditions are typical of all past field tests of UCG.

Cavity conditions depend upon the geohydrologic environment of the site and the UCG operating history. The cavity may be completely or partially full of rubble depending upon the nature of the overburden. If the overburden is consolidated material and has a high degree of structural integrity, the cavity is likely to be only partially filled with rubble. If the overburden is unconsolidated material and has no structural integrity, the cavity is likely to be completely full of rubble. The rubble mass in the cavity directly affects the amount of heat available for postburn coal pyrolysis because the energy stored in the mass is the energy source for that pyrolysis. The gasification operating pressure history may have either inhibited or promoted water influx into the cavity. The source of water influx can be the coal seam and/or the overburden. In addition, the postburn pressure in the cavity can be high or near atmospheric pressure depending upon whether the process wells are shut-in or open.

The simulation of postburn pyrolysis is modeled by reproducing a small cylinder-shaped element of the coal and rubble at the boundary between the rubble mass and the coal seam (Detail A, Figure 1). This element is considered one-dimensional and, in conjunction with a time-dependent temperature profile, will yield data useful for describing the rate and extent of postburn pyrolysis. Those cavity conditions which minimize the distance that the pyrolysis zone travels into the coal will tend to minimize the amount of contaminants generated.



FIELD SITUATION



DIFFERENTIAL ELEMENT FOR SIMULATION

Figure 1. Simulation of UCG Postburn Pyrolysis

Numerical Simulation

Model Formulation

Penetration of the pyrolysis zone into coal is modeled as an opposed combination of conductive and convective heat transport. Drying and pyrolysis zones develop in the coal as it is heated. Water involved in the drying process comes from connate water and water injection or influx. The model assumes that all water is vaporized at the wet coal-dry coal interface (steam front). Steam flows through the dry coal to the pyrolysis zone where it mixes with pyrolysis gases and reacts with the high temperature char. These vapors flow through the pyrolysis zone and enter the cavity, convectively cooling it.

Pressure drop is assumed to be negligible through the dry and pyrolyzed coal regions. Because subbituminous coals shrink and crack when dried and pyrolyzed, low resistance flow paths are formed in the high temperature coal zone. It is reasonable to assume that pressure drop through the pyrolysis and drying zones will be negligible and will be equal to the system pressure maintained at the coal cavity. Since it is assumed that the system pressure will be lower than the local hydrostatic pressure, flow will be from the coal aquifer to the drying interface.

The movement of fluids through the coal pore space and the accumulation of liquids (component concentrations) within the space are determined volumetrically. This technique is used because of the assumption of negligible pressure drop in the dry coal and pyrolysis zones and because water movement through the coal aquifer is specified by a flux term boundary condition. The mass of material produced from the pore space is the difference between the mass of material entering, converted to volume, and the volume of material that can exist in the pore. Vapor phase components are assumed to flow preferentially to water through the pore space since permeability to gas is much higher than that to liquid.

The following assumptions were made in order to simplify the model. (1) The model is one-dimensional cartesian. (2) The system is adiabatic. (3) Solid and fluid phases are at the same temperature. (4) The effect of coal fracturing on thermoconductivity is not handled explicitly in the model but is assumed to be compensated for by the conductivity-temperature relationships. (5) All pyrolysis products are produced in the vapor phase and do not condense within the reactor.

Model Equations

The model is formulated with conservation of mass equations for each mobil component and for the coal solid. An energy balance is written which accounts for heat transport through the solid and chemical heats of reaction within the coal from devolatilization and steam-char conversion. Convective heat transport of the mobil phases is also considered in conservation of the energy equation.

Three mass balance equations are used to describe the mobile components in the resource. Flux rates and masses of water, steam, and pyrolysis gases in the pore space are determined volumetrically. First, the total volume of material in the pore space is calculated by summing the liquid and vapor volumes entering the pore space with the material produced in the pore space from vaporization and pyrolysis. Second, the volume leaving is the difference between the total water and vapor and the maximum volume of material that can exist in the pore space at the specified system pressure. The volume leaving is converted to a mass by multiplying by the appropriate component densities. At the steam front, only vapor is produced from the pore space, unless water movement into the pore space exceeds the pore volume. Pyrolysis gas is the same as vapor components from devolatilization and steam-char reaction. For simplicity, it is assumed that no pyrolysis gas remains in the pore space.

The volume of material flowing through the coal pore space plus material previously in the pore is given by:

$$\text{Vol}_{wg} = (F_{wg} \Delta t)/\Delta x + (L_v \Delta t)/\Delta x + \rho_{wg} \quad (1)$$

$$\text{Vol}_{pg} = (F_{pg} \Delta t)/\Delta x + r_{sc} \Delta t/\gamma_{sc} + (r_d \Delta t)/\gamma_d \quad (2)$$

$$\text{Vol}_w = (F_w \Delta t)/\Delta x + \rho_w + W \quad (3)$$

The mass of material remaining in the pore space is determined volumetrically. Two cases are used for the concentration terms:

Case 1:

(Water volume less than total pore volume. All available water fills the pore space. No movement of water from the pore).

$$\rho_w = \text{Vol}_w \gamma_w \quad (4)$$

$$\rho_{pg} = 0 \quad (5)$$

$$\rho_{wg} = (\phi - \text{Vol}_w) \gamma_{wg} \quad (6)$$

Case 2:

(Water volume greater than total pore volume. No vapor remains in pore space. Excess water flows from pore).

$$\rho_w = \phi \rho_w \quad (7)$$

$$\rho_{pg} = 0 \quad (8)$$

$$\rho_{wg} = 0 \quad (9)$$

The material leaving the cell is now the total amount in the space minus the accumulation:

$$F_{wg} = (\text{Vol}_{wg} \gamma_{wg} - \rho_{wg}) (\Delta x / \Delta t) \quad (10)$$

$$F_{pg} = (r_{sc} + r_{pg}) \Delta x \quad (11)$$

$$F_w = (\text{Vol}_w \gamma_w - \rho_w) (\Delta x / \Delta t) \quad (12)$$

The volume and mass flux of pyrolysis gas (Vol_{pg} , F_{pg}) are the sum of the gases produced from devolatilization and steam-char reactions. An averaged devolatilization gas composition from previously acquired Hanna coal pyrolysis data (Miknis 1986) is used.

In the model, coal is assumed to be composed of four weight fractions: fixed carbon and ash (W_c), volatiles (W_v), and water (W_w). The weight fraction of ash is determined by difference. The coal heat capacity (C_p) and density (ρ) are mass-weighted sums of solid, volatile matter, water, steam, and pyrolysis gas components. The equation relating total heat capacity and density is as follows:

$$\rho C_p = (1 - W_w) \rho_s C_{p_c} + (\rho_w C_{p_w} + \rho_{pg} C_{p_{pg}} + \rho_{wg} C_{p_{wg}}) \quad (13)$$

Depletion of the volatile matter and char reduces the concentration of the coal solid (ρ_s). Kinetic expressions are used to describe the devolatilization (Britten 1986) and steam-char (Taylor 1976) reactions. The expressions for change in coal concentration are given by:

$$\rho_s = \rho_v + \rho_c \quad (14)$$

$$\frac{\partial \rho_v}{\partial t} = -r_d \quad (15)$$

$$\frac{\partial \rho_c}{\partial t} = -r_{sc} \quad (16)$$

where,

$$r_d = 198 \times 10^3 \rho_v e^{(-9070/(T+460))} \quad (17)$$

$$r_{sc} = 9.386 \times 10^8 \rho_c (PY_w)^{.5} e^{(-39852/(T+460))} \quad (18)$$

The energy balance equation for the coal resource involves conduction from the rubble into the coal, vaporization of water, heats of reaction for devolatilization and steam-char reactions, and convective heat transport from the produced vapors and injected water. The energy equation may be written as:

$$\rho C_p \frac{\partial T}{\partial t} = \frac{\partial}{\partial x} \left(k \frac{\partial T}{\partial x} \right) + \frac{\partial H}{\partial x} + (qr)_{sc} + (qr)_d + Q \quad (19)$$

At the steam front, the steam flux is determined by doing an energy balance with the quantity of steam vaporized being equal to the net heat transferred at the front:

$$L_V = \frac{1}{q_V} [(-k_{s+} \frac{\partial T}{\partial X})|_{s+} + (k_{s-} \frac{\partial T}{\partial X})|_{s-}] \quad (20)$$

The mass and energy balance equations are coupled by a convective heat flux term (H) which is the sum of the enthalpies times the respective mass fluxes of liquid and gas phase species flowing through the pore space. An averaged-molecular-weight and temperature-dependent enthalpy function is used for the pyrolysis gas products, and steam table data are used for liquid water and steam enthalpies.

Coal thermoconductivity (k) has two forms in the model: a constant value for wet coal (below vaporization) and a temperature-dependent conductivity for dry coal.

Numerical Solution

Equation 19 is solved as an initial value problem by using the method of lines (Sincovec 1975). Initial values for temperatures, water fraction, volatile fraction, and fixed carbon fraction must be specified, as well as water influx rate. The resource is divided into evenly spaced nodal points, and the temperature derivatives are discretized spatially using three point-centered differences, as are the convective term derivatives. The integration technique used is an implicit Euler's scheme. When the temperature at a node reaches vaporization temperature, it is maintained there until all of the water is vaporized. The rate of water vaporization is determined using equation 20.

The model outputs temperatures, liquid water pore saturation, gas pore saturation, the fraction of coal devolatilized, and the fraction of fixed carbon reacted.

Model Verification

The model will be verified by comparing its predicted pyrolysis zone penetration with actual data from WRI's contaminant control reactor. A heat loss term will be added to the model to facilitate comparison with laboratory data. The heat loss algorithm will not be used in field simulations since operating conditions there are near adiabatic.

Comparisons of the numerical model results with the experimental data will be performed using data from future experiments. Future work is currently scheduled that will include the verification of the numerical model after the heat loss term was added.

Information regarding numerical model nomenclature and parameters used is provided in Appendix A.

Physical Simulation

Postburn coal pyrolysis was simulated in a laboratory reactor using Hanna, Wyoming, coal samples taken parallel to the bedding plane. The samples used for testing were approximately 3 inches in diameter and one-foot long. Each sample was placed in the reactor vessel (Figure 2), allowing for simulation of the differential element on the cavity sidewall (Figure 1).

Reactor Design

The coal face is heated with hot inert gas plus a controlled quantity of oxygen injected through port H and exhausted through ports B and C (Figure 2). When the reaction temperature is achieved, a combustion zone develops at the coal face, and the hot-gas injection is terminated. Controlled cooling of the rubble zone simulates the heat transfer which would occur in the field. The rubble zone temperature is controlled by circulating hot gas through the tubing coil around the circumference of the rubble zone. Ports H_I and H_O are the coil inlet and outlet, and ports A and W are used to inject water into the coal and rubble zone. Thermocouples placed in the coal monitor the movement of the pyrolysis zone away from the simulated cavity sidewall during cooldown.

The laboratory reactor is designed to test the range of water influx conditions that can be encountered in a UCG field test. Both influx rates and sources (locations) of water influx can be varied. In addition, the pressure in the rubble zone and at the outer boundary of the coal can be varied. The control of water influx from each source and the control of pressure allow for the simulation of a variety of postburn conditions and potential operating procedures.

Reactor Material Selection

The selection of construction materials for the reactor is based upon the following temperature and pressure criteria: The designed maximum sustained temperature in the rubble zone is 1800°F (982°C), and the designed maximum pressure in the reactor is 250 psi. The heat exchanger in the rubble zone is assumed to maintain a constant 1800°F (982°C) temperature at the face of the rubble. The refractory is one-inch thick. Assuming that heat transfer from the outer surface of the reactor is by natural convection, the calculated skin temperature is 1167°F (630°C). The materials selected for the reactor are based upon the calculated skin temperature and maximum pressure. The shell of the vessel is constructed of 8-inch schedule 40, 304 stainless steel (SS) pipe. ANSI class 600# 304 SS flanges are used on both ends of the unit. The reactor vessel has an inner length of 36 inches. The process piping is 1/2-inch diameter 304 SS tubing (0.35-inch wall thickness). The thermocouples are 1/16-inch diameter 304 SS and are installed in the vessel through 1/4-inch NPT schedule 40 304 SS couplings welded to the shell.

Reactor Controls and Instrumentation

The piping and instrument diagram illustrates all manual and electrical controls for the reactor as well as the data acquisition requirements for the system (Figure 3). Temperature control of the rubble zone is achieved by circulating hot flue gas from a SS methanol burner (B-104) through the SS heat exchanger in the refractory surrounding the rubble zone. An electro-pneumatic control valve is used for adding nitrogen to the flue gas in order to achieve the desired gas temperature.

Another methanol burner (B-103) injects hot gases, with excess oxygen content, directly into the rubble zone and thus initiates combustion of the coal and subsequent development of the char face.

Water injection into the coal or the cavity is manually controlled; either constant flow (NV-50405 NV-503) or constant pressure injection (PR-505) is possible. Rotometers (FI-504 or FI-503) are provided to measure injected water flow, and pressure transducers (PT-504 or PT-603) monitor the injection pressure.

An automatically controlled volume of nitrogen (FCV-402) can be added to the product gas stream for the dual purpose of attemperating product gas temperatures (TC-608) and providing a means of checking the measured product gas flow (FT-611).

Gas cleanup is achieved by a single-pass, shell-and-tube heat exchanger (H-600) and a demister tank (H-601) installed after the product gas is expanded by flow through a backpressure regulator (PR-609). Produced water and pyrolysis liquids are collected and analyzed.

Experimental Procedure

The following experimental procedure for the physical simulations was determined after the two shakedown experiments using the laboratory equipment:

1. The rubble boundary is heated to a predetermined temperature. An initial rubble boundary temperature of 1800°F (982°C) was selected in order to prevent damage to the laboratory reactor.
2. Air is used to ignite the coal and is then injected into the rubble until the coal core reaches a temperature in excess of 1800°F (982°C).
3. When the core reaches the desired temperature, the air injection is discontinued. The conditions are adjusted to match the selected simulation conditions and water injection.
4. The desired temperature versus time profile in the rubble zone is maintained during the physical simulation which lasts 24 hours or until the temperature at the coal face is less than 500°F (260°C).

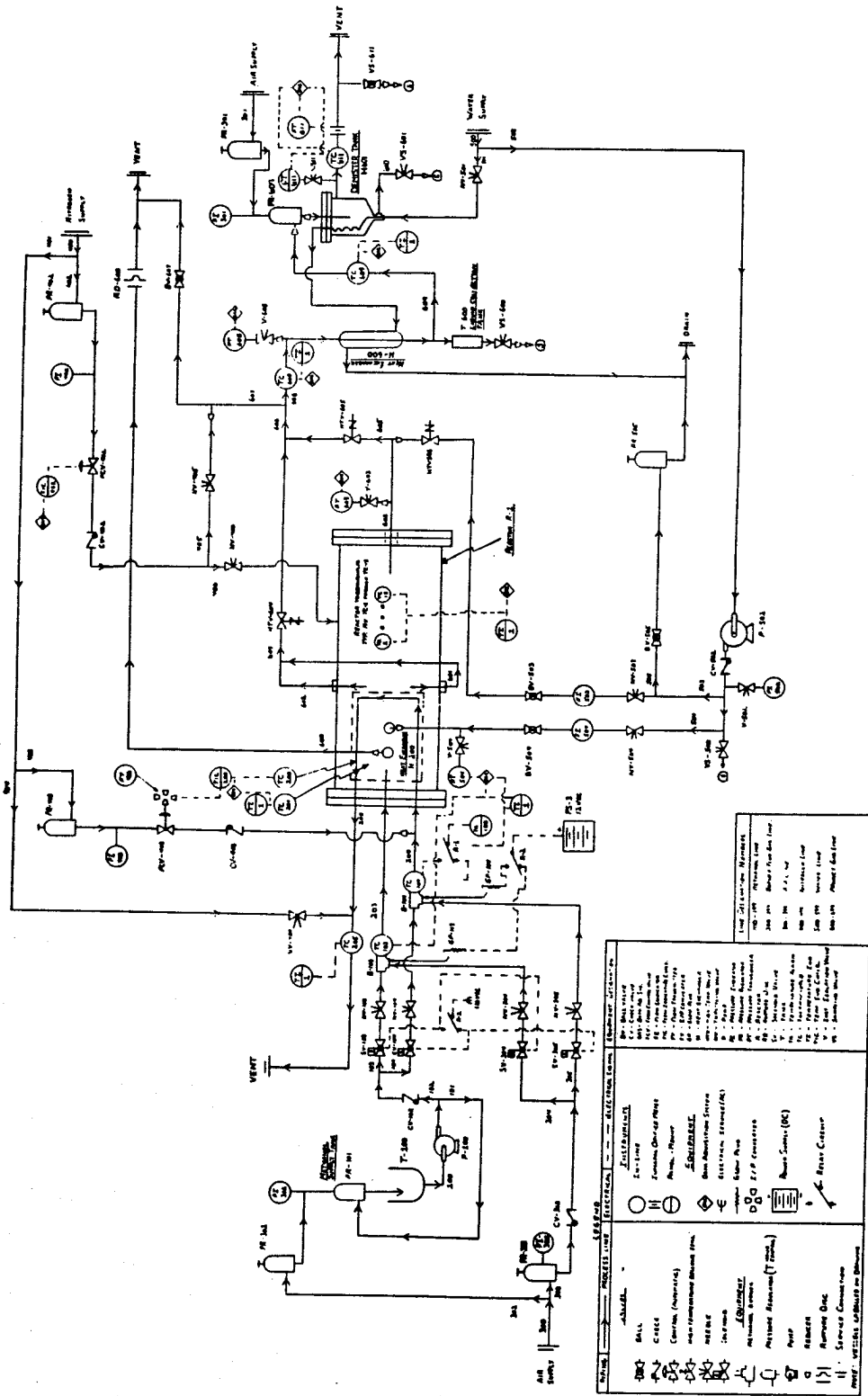


Figure 3. Contaminant Control Reactor Piping and Instrument Diagram

5. Coal samples are taken for analyses after the simulation reactor is shut down, cooled, and unloaded. Samples of liquids produced from the reactor are collected during the experiment. If water is injected during the experiment, samples of the injected water are taken during the water injection period. Also, hourly samples of the gases produced during the experiment are analyzed using gas chromatography.

Sampling and Analyses

A minimum of four coal samples are taken for analyses: initial (as received) sample, char sample, pyrolyzed sample, and unaltered sample. These coal samples are analyzed for proximate analyses, ultimate analyses, and water-soluble phenol concentration (Appendix B). Produced liquid samples are analyzed for a minimum of phenol concentration, sulfate concentration, ammonia concentration, and boron concentration.

If the quantity of produced liquids is sufficient, a full suite of analyses is performed on injected water samples and on produced liquids (Appendix B).

RESULTS AND DISCUSSION

Shakedown

Construction and installation of the contaminant control reactor were completed in August, 1986. An eight-hour trial test was completed for the purpose of testing equipment operation, process control, and process data acquisition. Two subsequent shakedown experiments were completed to test simulation procedures. In the first experiment, the rubble boundary was heated to 1800°F (982°C) and the coal face was ignited. The reactor was insulated and the rubble heat exchanger was shut off. The experiment lasted six hours after termination of ignition at which time the temperatures in the coal core were all below 500°F (260°C). No water was injected into the coal or rubble during this test, and the rubble zone was shut in. In the second experiment, the rubble was heated to 1800°F (982°C) and the coal was ignited. No insulation was placed on the reactor, but the rubble heat exchanger skin temperature was maintained at a temperature of 100°F (38°C) below the rubble temperature. This experiment lasted five hours after termination of ignition at which time the temperatures in the coal core were all below 500°F (260°C). Again, no water was injected into the coal or rubble; but, in this test, the rubble zone was vented to atmosphere.

The results of these shakedown tests confirmed the operability of the laboratory equipment, but the short duration of these dry experiments resulted in only a small amount of pyrolyzed coal. To increase the amount of pyrolyzed coal, it was decided to maintain the rubble heat exchanger surface at a temperature of 100°F (38°C) above the measured rubble temperature. For the remaining six experiments, the heat exchanger surface temperature set point was manually adjusted every half hour.

Initial Series of Physical Simulations

The initial series of six physical simulations for UCG postburn coal pyrolysis was designed to determine the effects of three variables on postburn coal pyrolysis and the subsequent contaminant generation and migration:

1. Pressure gradient direction in the coal seam: Pressure gradient direction is important in determining fluid transport in or out of the cavity.
2. Water influx rate through the coal seam: Preliminary numerical model indications show that the rate of water influx through the coal is a key factor affecting the pyrolysis zone penetration. Water influx through the coal is also important in the containment of generated contaminants.
3. Water influx into the cavity: Water influx into the cavity should result in lower cavity temperatures.

After the first two trial experiments, the remaining six experiments were conducted with varying conditions. The first three evaluated water injection into the cavity, and the last three evaluated water influx through the coal (Table 1). For the cavity water injection

**Table 1. Postburn UCG Coal Pyrolysis Physical Simulation
Experimental Conditions and Pyrolysis Zone Penetration**

<u>Rate of Water Injection</u>	<u>Test Conditions</u>	<u>Max. Penetration Depth</u>
0.1 cc/min.	Cavity Water Injection- Cavity Shut-in	0.53"
1.0 cc/min.	Cavity Water Injection- Cavity Shut-in	0.38"
1.0 cc/min.	Cavity Water Injection- Cavity Vented	0.59"
4.0 cc/min.	Water Injection through Coal- Cavity Vented	0.21"
0.16 cc/min.	Water Injection through Coal- Cavity Vented	0.31"
1.60 cc/min.	Water Injection through Coal- Cavity Vented	0.28"

simulations, two experiments were conducted with the cavity shut-in. The water injection rate is varied by an order of magnitude between the two tests to illustrate the impact of the injection rate. The other cavity water injection simulation was conducted with the cavity vented and a water injection rate equal to the higher injection rate of the two tests with the cavity shut-in. The cavity was vented for the three simulations of water injection through the coal. Three different water injection rates through the coal were used to illustrate the effect of water influx through the coal on the extent of postburn UCG coal pyrolysis.

This series of simulations was intended to answer the following questions:

1. Can postburn coal pyrolysis be reduced by injecting water into the cavity and/or by inducing water influx through the coal seam?
2. What is the source of specific contaminant species (i.e., which contaminants come from the coal seam)?
3. Are gaseous and liquid pyrolysis products the main source of phenolic contamination, or is the thermally altered coal and char a significant source of contamination?

Simulation Results

Pyrolysis Zone Penetration

Temperature profiles of the coal core are used to determine the maximum penetration depth of the pyrolysis zone. The varying penetrations of these six experiments are compared to determine the relative effectiveness of test conditions in limiting postburn pyrolysis. Based on gas analysis, the selected temperature of 500°F (260°C) is where significant pyrolysis of the coal begins.

Three temperature profiles of the coal core during experiment 7 are illustrated in Figure 4. The initial temperature profile at the termination of coal combustion is curve "1"; the temperature profile at the time of maximum penetration is curve "2"; and the final temperature profile when the coal face cools below 500°F (260°C) is curve "3." Maximum penetration of the pyrolysis zone (500°F/260°C) occurred at 0.59 inches, and minimum penetration occurred at 0.28 inches (Table 1). Appendix C provides the data similar to that in Figure 4 for each of the six experiments.

Data for experiments 6, 7, and 8 illustrate the relationship between the rate of water injection through the coal and the pyrolysis zone penetration (Figure 5). The higher the rate of water injection through the coal, the less the pyrolysis zone penetration.

When the core was removed from the reactor after experiments 6, 7, and 8, some valuable observations were made. In each test with water injection through the coal core, substantial radial flow of water out of the coal core and through the refractory casting was observed in the

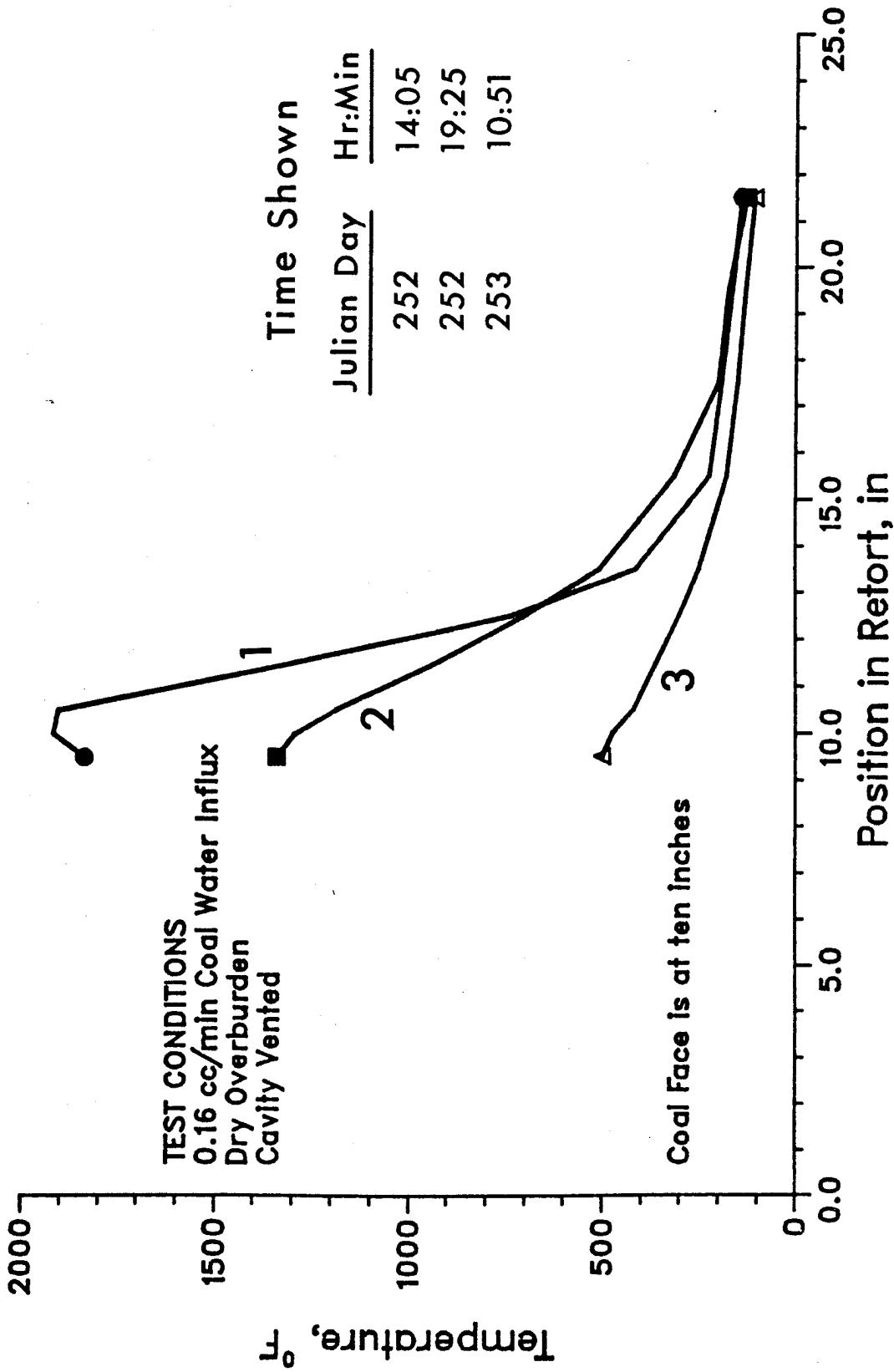


Figure 4. Temperature Profiles of Coal Core for Experiment No. 7

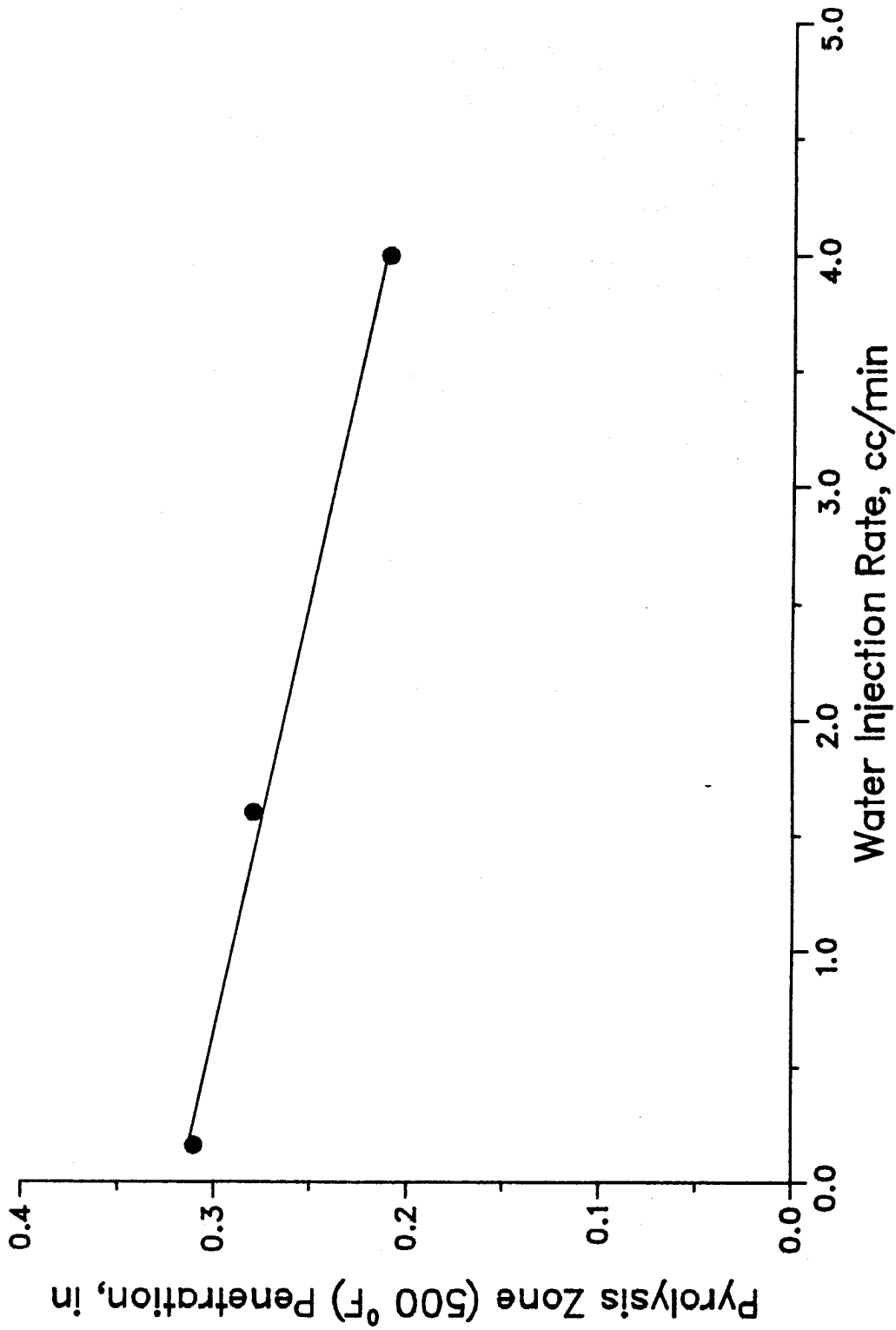


Figure 5. Pyrolysis Zone Penetration Versus Rate of Water Injection Through Coal with Cavity Vented

portion of the core below steam temperatures. The previously measured permeability of the refractory at these temperatures was on the order of 0.1 millidarcys (md). This permeability is at least an order of magnitude less than that already published for Hanna No. 1 coal (Hutchinson et al. 1977). This observation indicates that as steam is generated in the coal pores, the volume expansion creates a considerable impedance to water flow through the hot coal. This phenomenon may limit water influx through the coal seam in field conditions.

The results of the two cavity shut-in experiments indicate that higher water influx into the cavity will limit postburn pyrolysis (Figure 6). However, the data for the experiment in which the cavity was vented do not indicate any cooling of the rubble or coal face as a result of injected water. In the cavity shut-in experiments, steam generated from the water injected into the cavity was forced to disperse and flow through the coal core, while the steam in the cavity-vented experiment took the path of least resistance and flowed out of the rubble zone, thus cooling only a local region of rubble. Without significant cooling of the rubble zone or the coal face, the pyrolysis zone penetration was not reduced. In a field situation, channeling the water injected into a UCG cavity is possible, especially in cavities with a high-void volume.

Contaminant Production and Migration

The results in this section are presented in order-of-magnitude estimates of contaminant production for the following reasons:

1. Quantities of contaminants generated are small; in most cases, concentrations of these contaminants in the samples are near detection limits.
2. Losses in liquid sample recovery are significant due to the small mass of contaminants generated.

The data for experiment 3 illustrate that as pyrolysis of the coal occurs, the concentration of the water-soluble phenols weakly bound to the coal increases until the coal is completely pyrolyzed (Figure 7). Charred regions of the coal core have low concentrations of water-soluble phenols if the pyrolysis products generated in the core don't flow through the char zone. If the pyrolysis products flow through the char zone as in experiment 5 (Figure 8), the char tends to reabsorb phenols. If water also flows through the char zone, the amount reabsorbed on the char is reduced (experiments 6, 7, and 8). Appendix D provides the data similar to that in Figure 8 for each of the other four experiments.

The concentration of phenols found in the produced liquids is much greater than the concentration of phenols found on the thermally altered coal. The dilution of the phenol concentration by injected water is illustrated by the data in Table 2. There are multiple volumes for experiments 6 and 8 because sufficient volumes of samples were generated to determine the phenol concentration change with time in the produced liquid. The first value presented is for the first bottle of sample collected, the second value for the second volume of sample, and so on.

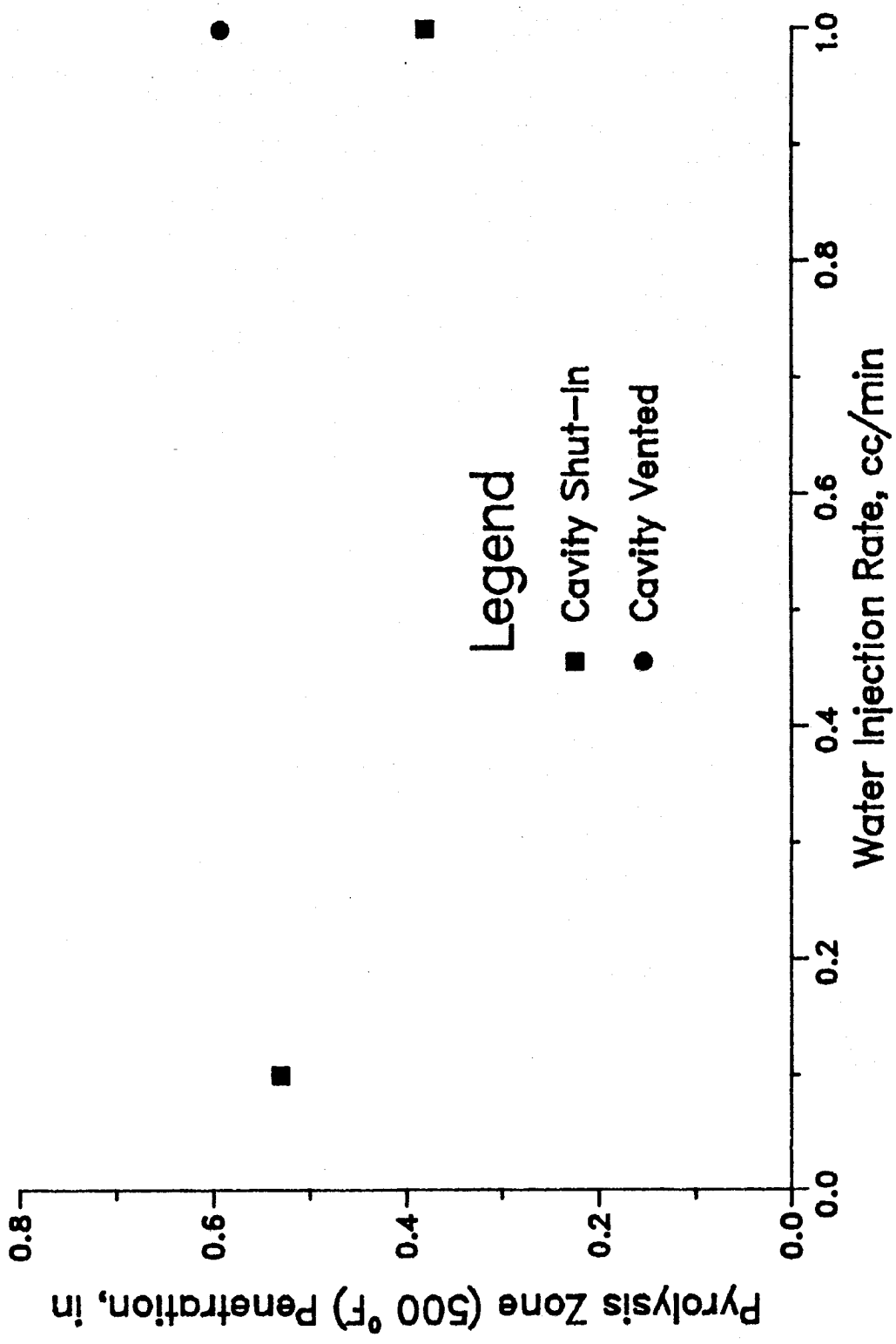


Figure 6. Pyrolysis Zone Penetration Versus Rate of Water Injection Into Cavity

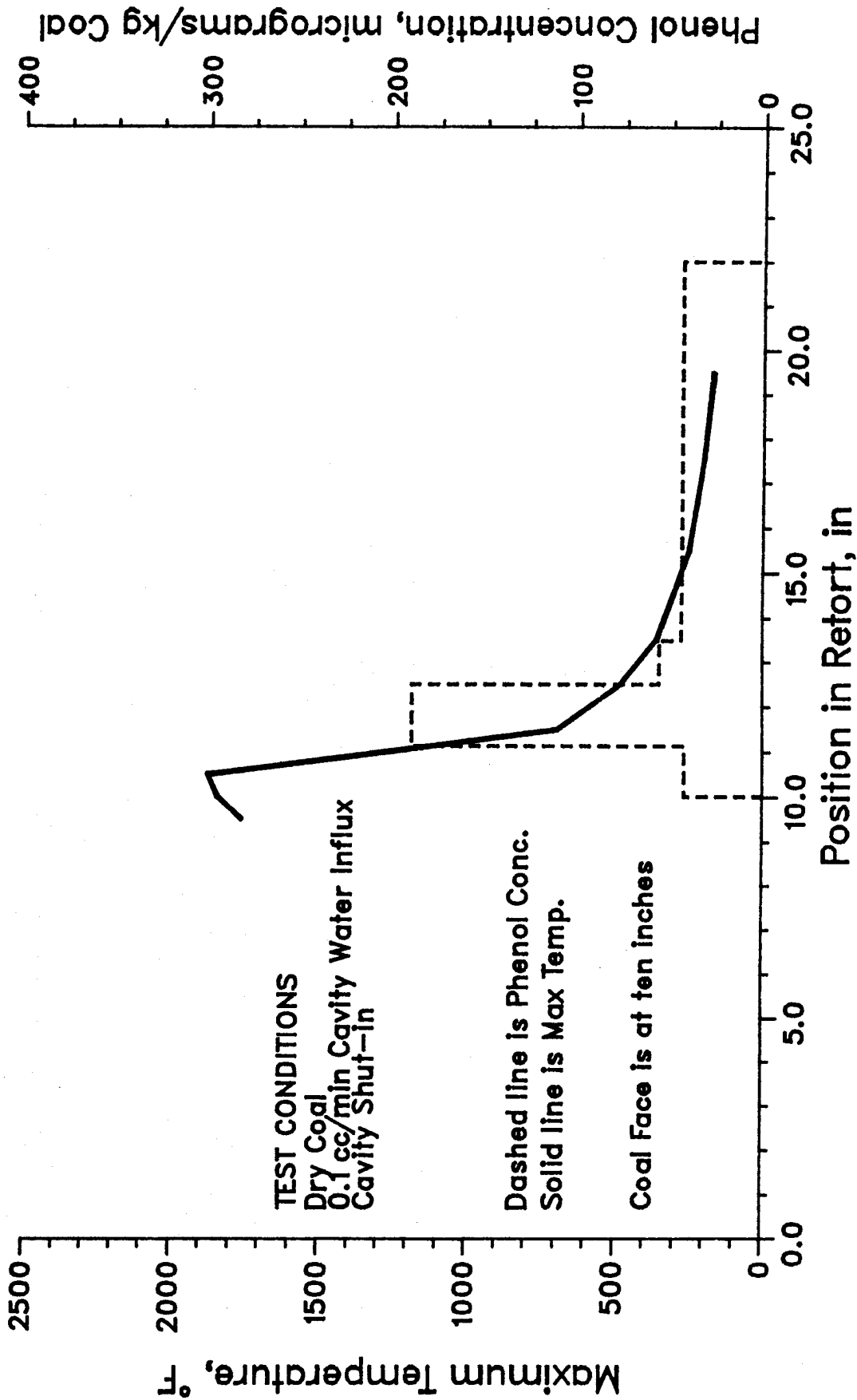


Figure 7. Maximum Temperature and Phenol Concentration Versus Position for Experiment No. 3

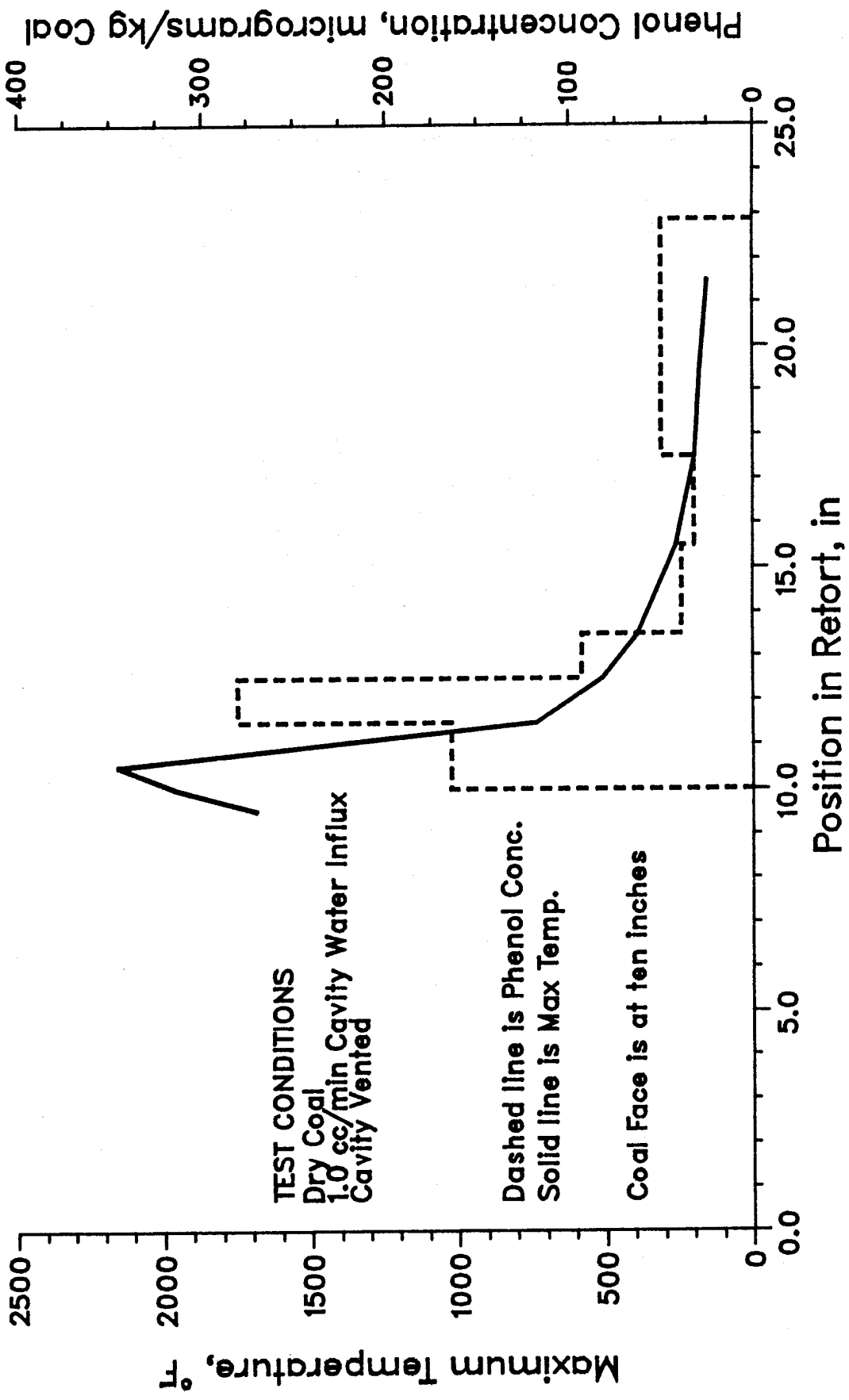


Figure 8. Maximum Temperature and Phenol Concentration Versus Position for Experiment No. 5

The value in parentheses for experiment 6 is a composite of the five samples.

The mass of phenols in the produced liquids is several orders of magnitude greater than the water-soluble phenols remaining on the coal (Table 3). Therefore, phenols are generated when the coal is pyrolyzed, and these contaminants migrate predominantly with the liquid and gaseous pyrolysis products. The amount of phenols that migrate with the pyrolysis products is much greater than the amount that remains on the thermally altered coal.

Table 2. Phenol Concentrations of the Liquids Produced During the Physical Simulations

Experiment #	Injection Rate cc/min	Phenols in Produced Liquid (mg/L)
3	0.1	650
4	1.0	N.D. ^a
5	1.0	210
6	4.0	51, 6.1, 2.1, 2.5, 2.3, (11)
7	0.16	1100
8	1.6	130, 58, 6.2

^a No data (sample container broken).

Table 3. Phenol Distribution Between the Coal and Produced Liquids

Experiment #	Injection Rate cc/min	Residual Phenols On Coal μg	Phenols in Produced Liquid μg
3	0.1	106	40,000
4	1.0	116	N.D. ^a
5	1.0	118	77,000
6	4.0	43	25,000
7	0.16	73	61,000
8	1.6	77	34,000

^a No data (sample container broken).

Per mass of coal pyrolyzed, the other contaminants found in the produced liquids during the simulations were calculated from the concentration of the species found in the liquid produced, the volume of liquid produced, and the mass of coal pyrolyzed during the simulation. The data used to determine the mass of species in the produced liquid (Appendix E) and the pyrolysis zone penetration (Table 1) together produce the results (Table 4) that illustrate the range of values for the mass of the individual species generated per mass of pyrolyzed coal. The variation of results is significant; but, it is evident that these contaminant species have a source from the coal seam, are mobilized when coal is pyrolyzed, and migrate with the coal pyrolysis products. The contaminants which exhibit this behavior are the organic contaminants

Table 4. Other Contaminant Species Generated During Coal Pyrolysis

Contaminant Species	Mass of Species in Produced Liquids Mass of Coal Pyrolyzed	
	Lowest Value ^a	Highest Value ^a
Total Organic Carbon (mg/kg)	2900	4700
Sulfate (mg/kg) ^b	300	4800
Ammonia (mg/kg)	400	1600
Boron (µg/kg)	80	2800
Fluoride (mg/kg)	20	130
Barium (µg/kg)	90	8900
Arsenic (µg/kg)	Trace (<20)	700
Selenium (µg/kg)	Trace (<50)	120 (<360)
Lead (µg/kg)	70	4300

^a Reported lowest and highest values based on comparison of results from experiments 3, 5, 6, 7, & 8. Values are presented to confirm contaminant species origin from coal pyrolyzes.

^b Values reported for ammonia represent the mass of nitrogen in the ammonia.

contributing to the measured total organic carbon concentration, sulfates, ammonia, boron, fluoride, barium, arsenic, selenium, and lead. (The amount of these contaminant species remaining on the coal was not determined in this research.)

CONCLUSIONS

Experimental Conclusions

The following conclusions are drawn from the results of the initial series of physical simulations:

1. Liquid and gaseous pyrolysis products are a major source of phenols in groundwater when compared to thermally altered coal. Phenols in produced liquids are more than an order of magnitude greater than those water-soluble phenols remaining on the coal.
2. Most contaminant species associated with UCG operations are present in the pyrolysis products. Analyses of produced liquids show the presence of phenols, ammonia, sulfates, arsenic, boron, barium, fluoride, lead, and selenium.
3. Injection of water into the cavity can limit postburn pyrolysis, but only to the degree that channeling does not affect the overall cooling of the cavity.
4. Water flow through the coal will limit postburn pyrolysis, but steam generation in the coal appears to limit the rate of water flow.

Recommendations for UCG Field Testing

The conclusions drawn from the analyses of experimental results were used to formulate recommendations for operation of the upcoming Rocky Mountain 1 UCG Field Demonstration scheduled for the last quarter of 1987. The following recommendations are made for all future UCG field testing to minimize groundwater contamination and promote containment of contaminants near the UCG cavity.

1. The flow of pyrolysis liquids and gases into the underground formation should be prevented by minimizing gas leakage to the formation during gasification and venting the cavity as soon as the gasification process is complete. Also, water injected into the cavity after UCG operations must not generate steam pressures greater than the hydrostatic pressure of the coal seam or connected aquifers, or postburn pyrolysis liquids and gases will flow into the underground formation.
2. Although preliminary results indicate that water influx from the coal seam is beneficial, it may be difficult to achieve an influx rate higher than the natural influx rate. Therefore, water injection wells surrounding the cavity are not expected to increase the water influx rate.

Current Research

The results of this research have led to additional research at the Western Research Institute (WRI). The following activities are currently in progress or scheduled in the near future:

1. The Gas Research Institute has sponsored more detailed research related to UCG postburn pyrolysis. A refractory heat transport term was incorporated into the numerical model to numerically simulate the experimental data. The numerical

model will be verified using the experimental results of this series of experiments.

2. The United States Department of Energy (DOE) UCG Program has sponsored complementary research related to UCG postburn pyrolysis.
3. The DOE Advanced Process Technology Program has sponsored preliminary research investigating pyrolysis occurring after tar sands and oil shale thermal extraction processes.
4. The DOE Advanced Process Technology Program has sponsored detailed geochemical analysis to determine the fate of contaminant species resulting from UCG.

ACKNOWLEDGMENTS

The authors express thanks and appreciation to the United States Department of Energy for funding of this work under Cooperative Agreement Number DE-FC21-83FE60177. Special thanks are given to (1) the lead technicians for this project: Paul Paisley, Mark Lyons, and Ron Beckett and (2) the research manager: David Sheesley. The data presented in this paper are a result of their conscientiousness and hard work.

DISCLAIMER

Mention of specific brand names or models of equipment is for information only and does not imply endorsement of any particular brand.

REFERENCES

- Ahner, P. F. "Rawlins Test 2 Data Analysis," Eighth Underground Coal Conversion Symposium Proceedings, Keystone, CO, 1982.
- Badzoich, S., D. R. Gregory, and M. A. Field. "Investigation of the Temperature Variation of the Thermal Conductivity and Thermal Diffusivity of Coal," Fuel, 1964, 43, 267-280.
- Britten, Jerald. "Recession of a Coal Face Exposed to a High Temperature," Int. J. Heat Mass Transfer, 1986, 29, 965-978.
- Cooke, S. D., and R. L. Oliver. "Summary of the Groundwater Monitoring Program at the Hanna, Wyoming Underground Coal Gasification Test Sites," U.S. Department of Energy Technical Note, DOE/METC-85/4006, July 1985.
- Covell, J., L. F. Wojdac, F. A. Barbour, G. W. Gardner, R. Glass, and P. J. Hommert. "Results of the Fourth Hanna Field Test," Sixth Annual Underground Coal Conversion Symposium Proceedings, Shangri-la, OK, 1980.
- Glaser, R. R., and T. E. Owen. "Postburn Generation, Control, and Recovery of Organic Compounds in Underground Coal Gasification," Western Research Institute Topical Report. Prepared for the Gas Research Institute, January 1986.
- Hill, R. W., C. B. Thorsness, R. J. Cena, W. R. Aiman, and D. R. Stephens. "Results from the Third LLL Underground Coal Gasification Experiment at Hoe Creek," Sixth Annual Underground Coal Conversion Symposium Proceedings, Shangri-la, OK, 1980.
- Hutchinson, H. L., R. M. Boyd, and D. D. Fischer. "Hydrologic Characterization for Hanna III," Third Annual Underground Coal Conversion Symposium Proceedings, Fallen Leaf Lake, CA, 1977.
- Miknis, F. P., F. T. Turner, and G. L. Berdan. "Isothermal Pyrolysis of Hanna Coal," Western Research Institute, Laramie, WY, December 1985, DOE/FE/60177-2214.
- Oliver, R. L. "Final Results of the Tono 1 UCG Cavity Excavation Project, Centralia, Washington," Sept. 1986, Western Research Topical Report. Prepared for the Lawrence Livermore National Laboratory.
- Taylor, R. W., and D. W. Bowen. "Rate of Reaction of Steam With Carbon," Lawrence Livermore National Laboratory, 1976, Report UCRL-52002.

**APPENDIX A. NOMENCLATURE AND VALUES FOR PARAMETERS
USED IN THE NUMERICAL MODEL**

Symbols

C_p	Specific heat (Btu/lb-°F)
F_i	Mass flux of component i (lb/hr-ft ² reservoir)
F_Q	Water injection source term (lb/hr-ft ² reservoir)
H	Convective heat flux (Btu/hr-ft ² reservoir)
HL	Steady state heat loss from refractory grout to surroundings (Btu/hr-ft ³ reservoir)
HT	Heat transport between refractory grout and coal (Btu/hr-ft ³ reservoir)
h_i	Enthalpy of component i (Btu/lb)
k	Thermal conductivity (Btu/hr-ft-°F)
L	Total axial length of coal core (ft)
L_v	Steam flux (lbs/hr-ft ²)
P	System pressure (PSIA)
Q	Water injection source term (lbs/hr-ft ³ reservoir)
q_i	Heat of reaction (Btu/lb)
q_v	Latent heat of vaporization of water (Btu/lb)
r	Reaction rate (lbs/hr-ft ³ reservoir)
t	Time (hrs)
T	Temperature (°F)
W_i	Weight fraction of component in coal
x	Axial distance (ft)
Y_i	Mole fraction of component i in the vapor phase

Greek Symbols

ρ_i	Concentration of component i (lb/ft ³ reservoir)
ϕ	Porosity
γ_i	Density of component i (lb/ft ³)

Subscripts

c carbon
d devolatilization
g refractory grout
pg pyrolysis gas
s coal solid
sc steam char
s+ zone above vaporization temperature
s- zone below vaporization temperature
v volatile matter
w water
wg steam

Parameter Values Used in Calculations

1. Water and Steam

$$\rho_w, \rho_{wg}, C_{p_w}, C_{p_{wg}}, h_w, h_{wg}, q_v \quad \text{Steam table data}$$

2. Pyrolysis data

$$Y_w = .57$$

$$MW_{pg} = 36$$

$$h_{pg} = .394 + (2.25 \times 10^{-4} T)$$

3. Heats of reaction

$$q_{sc} = -4437.$$

$$q_d = 0.$$

4. Coal properties

$$k_{s-} = .23$$

$$k_{s+} = .578 (-.15 + 3.03 \times 10^{-3} TK - 6.54 \times 10^{-6} TK^2 + 4.51 \times 10^{-9} TK^3)$$

$$TK = (T+460)/1.8$$

(Badzoich 1964)

APPENDIX B. EXPERIMENTAL CHEMICAL ANALYSES

**Procedures for Analyses of Water-Soluble Phenols
Concentration of Coal Samples**

The following procedure is used for analyzing the concentration of water-soluble phenols in the coal and thermally altered coal samples:

1. weigh 5 g of the crushed coal sample into a teflon-lined vial;
2. add 20 ml of deionized water to the vial;
3. shake vigorously and shake at least once per day for five days;
4. filter the slurry through a 1.2 μ glass fiber filter; rinse the coal sample with deionized water while filtering until the volume of extract is 25 ml;
5. add 1 or 2 drops of H_3PO_4 to the extract to preserve the sample; and
6. use EPA method 420.2 for phenol analysis of the extract.

Notes: Express results in μ g phenols per kg sample. The detection limit for this procedure is about 10 μ g/kg phenols.

**Table B-1. Full Suite of Analyses for Produced Liquids
and Injected Water**

Parameter	Analytical Method
Trace Elements	
Aluminum	EPA Method No. 200.7
Antimony	EPA Method No. 200.7
Arsenic	EPA Method No. 206.2
Barium	EPA Method No. 200.7
Beryllium	EPA Method No. 200.7
Boron	EPA Method No. 200.7
Cadium	EPA Method No. 200.7
Calcium	EPA Method No. 200.7
Chromium	EPA Method No. 200.7
Cobalt	EPA Method No. 200.7
Copper	EPA Method No. 200.7
Iron	EPA Method No. 200.7
Lead	EPA Method No. 239.1
Magnesium	EPA Method No. 200.7
Manganese	EPA Method No. 200.7
Mercury	EPA Method No. 245.1
Nickel	EPA Method No. 200.7
Potassium	EPA Method No. 200.7
Selenium	EPA Method No. 270.2
Silver	EPA Method No. 200.7
Sodium	EPA Method No. 200.7
Thallium	EPA Method No. 279.2
Vanadium	EPA Method No. 200.7
Zinc	EPA Method No. 200.7
Total Organic Carbon (TOC)	Coulometrics, Inc. Analyzer
Total Mineral Carbon (TMC)	Coulometrics, Inc. Analyzer
Dissolved Organic Carbon (DOC)	Coulometrics, Inc. Analyzer
Dissolved Mineral Carbon	Coulometrics, Inc. Analyzer
Alkalinity	EPA Method No. 310.1
pH	EPA Method No. 150.1
Conductivity	EPA Method No. 120.1
Chemical Oxygen Demand (COD)	Reactor Digestion Method
Total Dissolved Solids (TDS)	ASTM Method D 1888-67
Total Suspended Solids (TSS)	ASTM Method D 1888-67
Total Kjeldahl Nitrogen (TKN)	EPA Method No. 351.2

**Table B-1. Full Suite of Analyses for Produced Liquids
and Injected Water (continued)**

Parameter	Analytical Method
Ammonia	EPA Method 351.2 manifold on Technician AAI Analyzer
Chloride	EPA Method No. 325.3
Fluoride	EPA Method No. 340.2
Cyanide (total)	EPA Method No. 335.2
Sulfate	EPA Method No. 375.4
Phenols	EPA Method No. 420.2

APPENDIX C: EXPERIMENTAL TEMPERATURE DATA

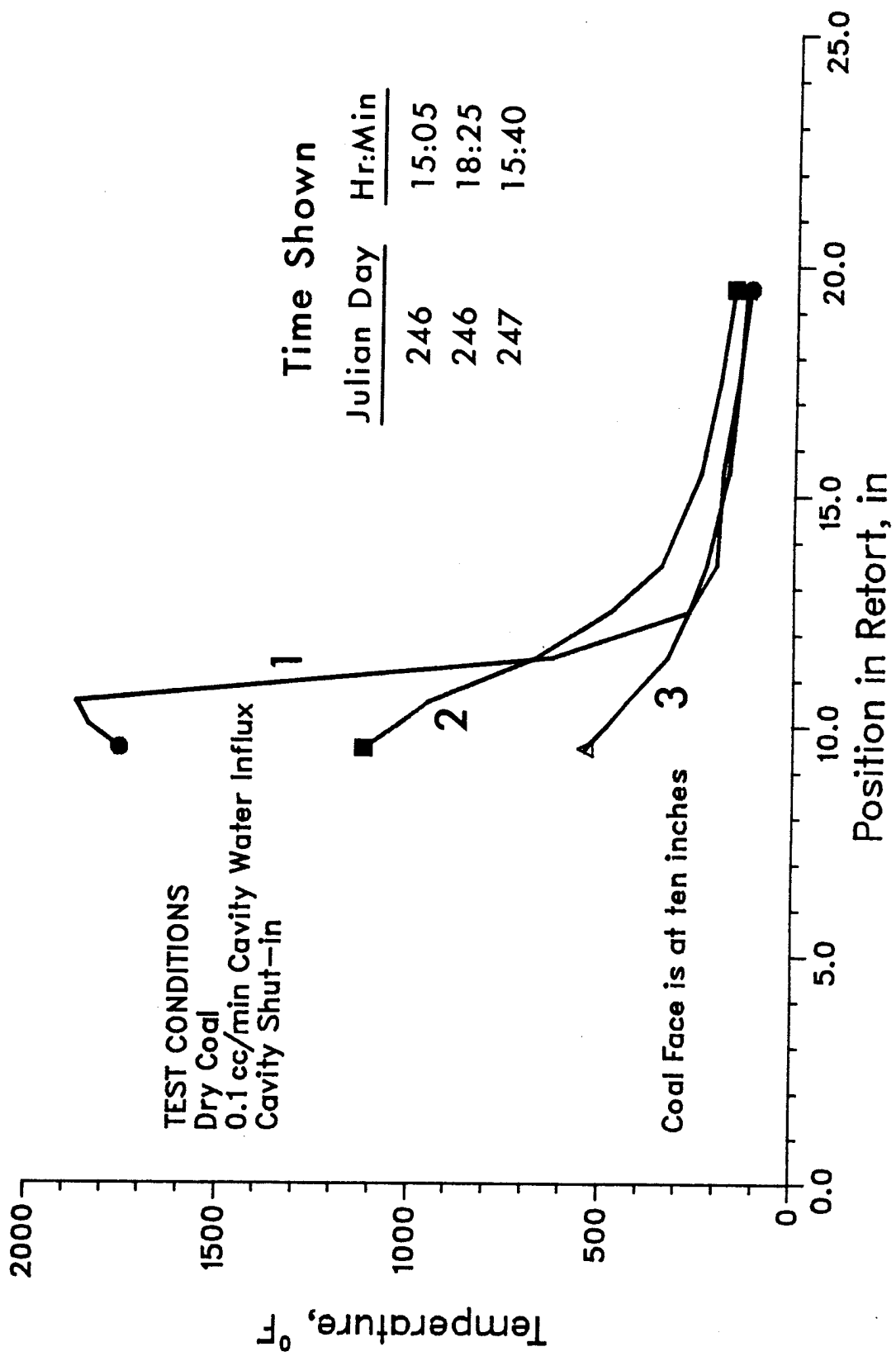


Figure C-1. Temperature Profiles of Coal Core for Experiment No. 3

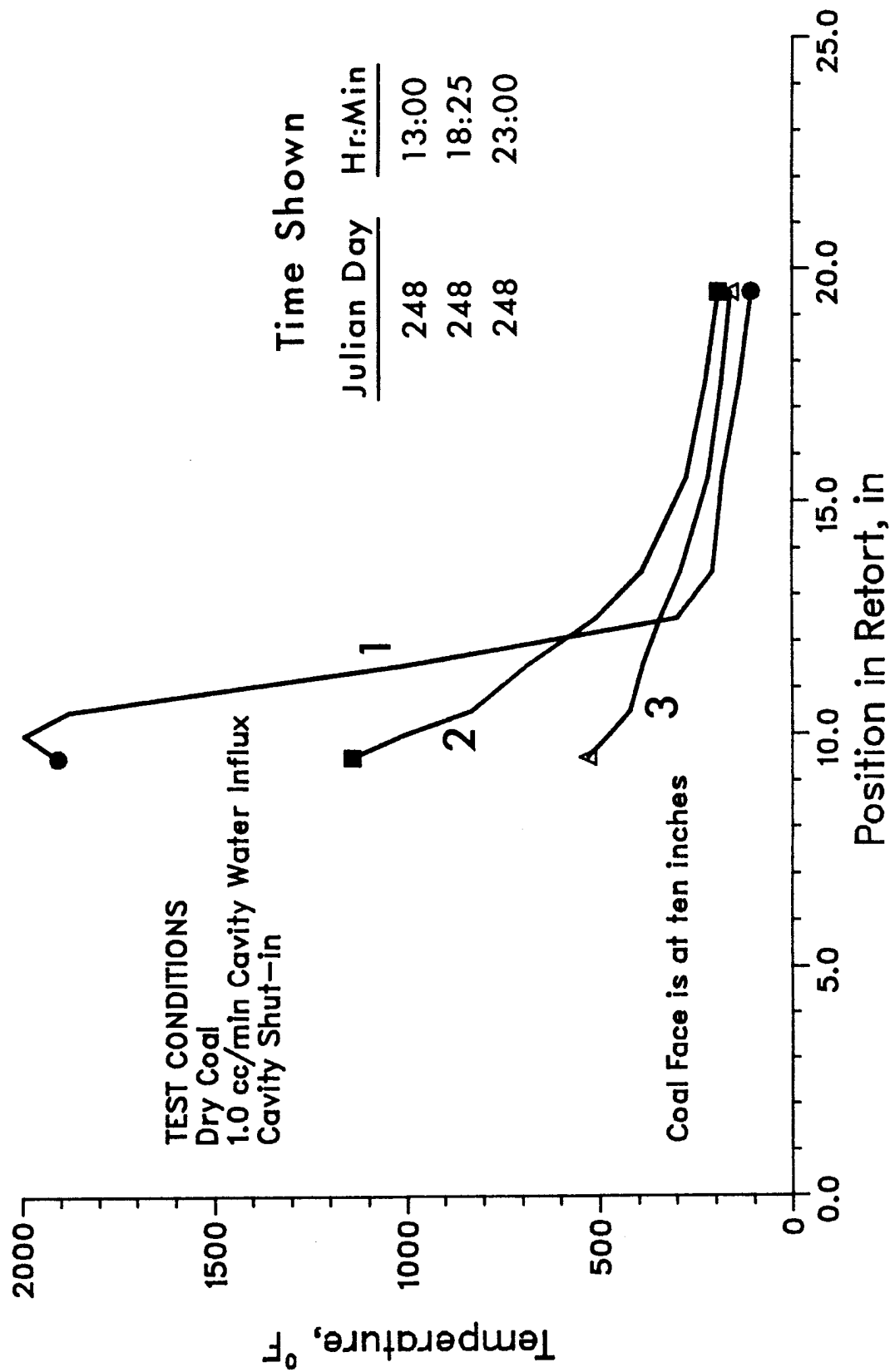


Figure C-2. Temperature Profiles of Coal Core for Experiment No. 4

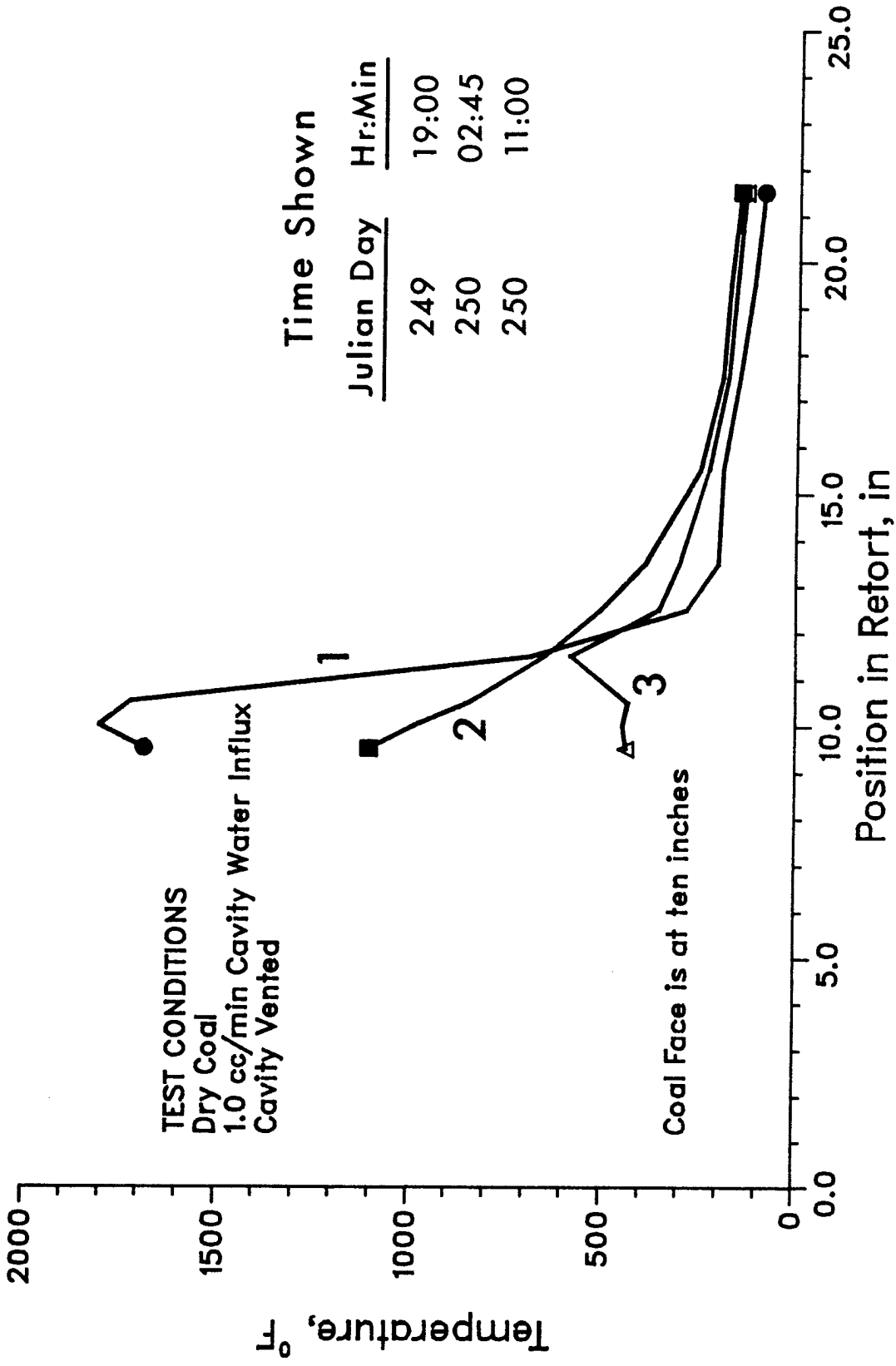


Figure C-3. Temperature Profiles of Coal Core for Experiment No. 5

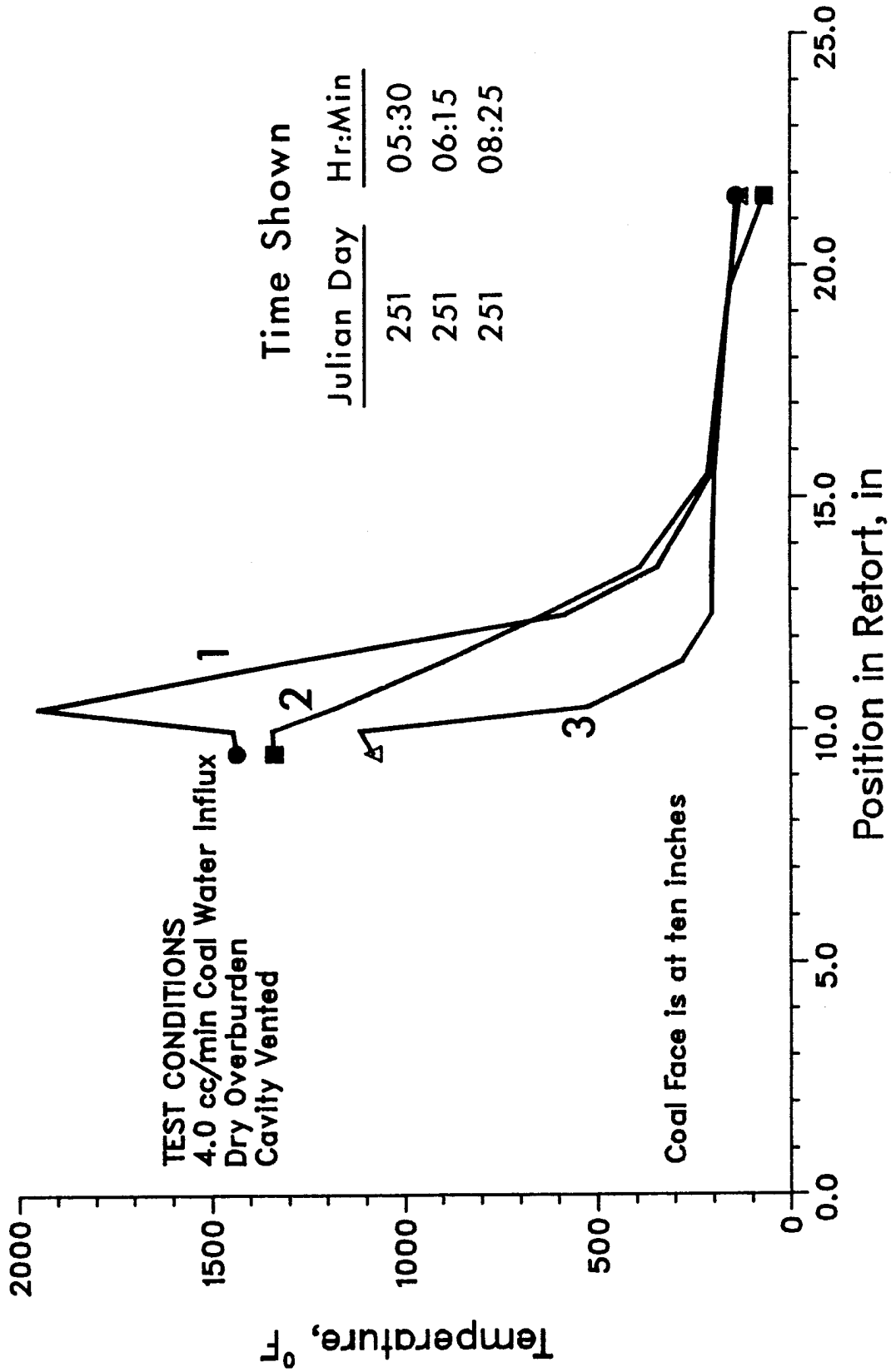


Figure C-4. Temperature Profiles of Coal Core for Experiment No. 6

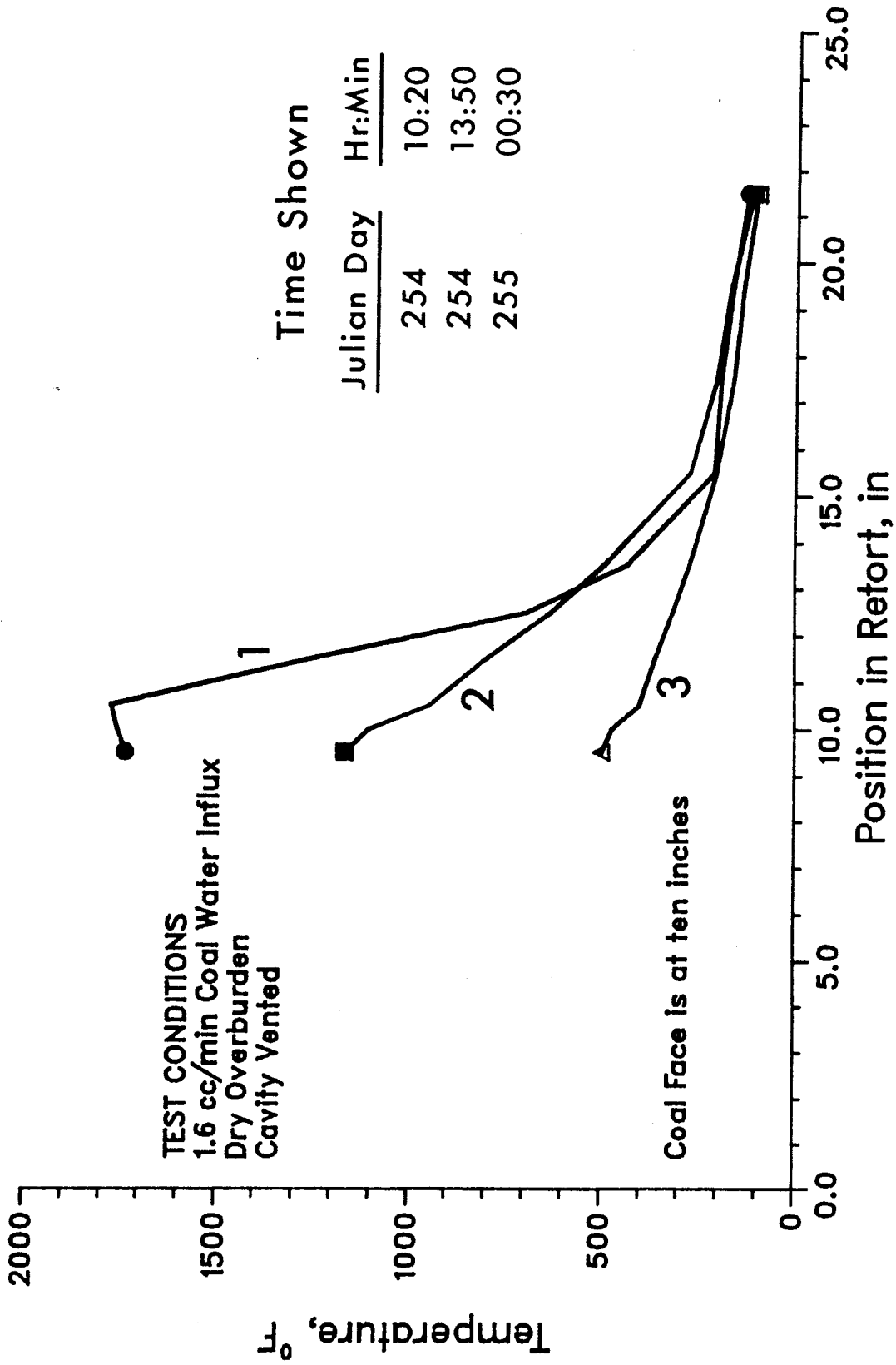


Figure C-5. Temperature Profiles of Coal Core for Experiment No. 8

APPENDIX D: EXPERIMENTAL DATA FOR PHENOLS

Table D-1. Phenol Concentrations of Coal Samples

Experiment #	Coal Description	Zone Weight (Grams)	Avg. Max. Temp. of Zone (°F)	Water Soluble Phenol Concentration (µg/kg)
3	As Received (AR)	1908	---	44
	Char (C)	95	1285	42
	Pyrolyzed (P)	176	590	190
	Unaltered (U)-1	142	420	56
	U-2	1372	265	44
4	AR	1927	---	34
	C	91	1530	78
	P-1	123	780	360
	P-2	134	450	69
	P-3	305	335	38
	U-1	361	255	36
	U-2	192	210	42
	U-3	522	190	43
5	AR	1871	---	35
	C	119	1350	164
	P-1	91	620	280
	P-2	136	450	93
	P-3	257	330	39
	U-1	243	230	32
	U-2	415	175	50
	U-3	435	175	50
6	AR	1890	---	31
	C	148	1335	41
	P	217	755	180
	U-1	288	315	47
	U-2	1059	180	32
7	AR	1884	---	37
	C	206	1420	52
	P-1	147	650	170
	P-2	232	415	50
	P-3	310	260	21
	U-1	352	190	24
	U-2	201	160	27
	U-3	205	160	28
8	AR	1936	---	35
	C	80	2225	48
	P-1	116	1590	120
	P-2	119	625	170
	U-1	592	360	34
	U-2	793	170	24

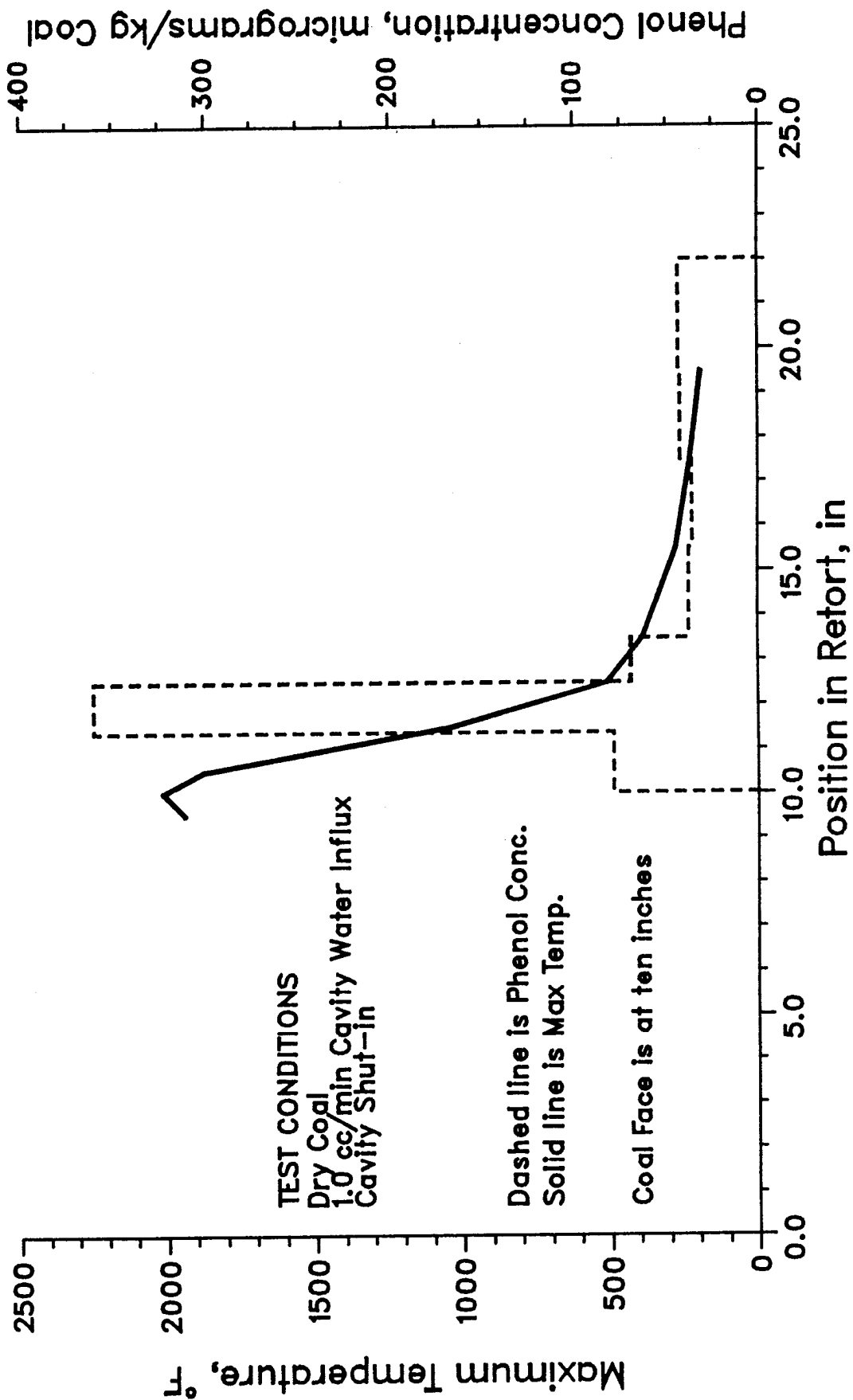


Figure D-1. Maximum Temperature and Phenol Concentration Versus Position for Experiment No. 4

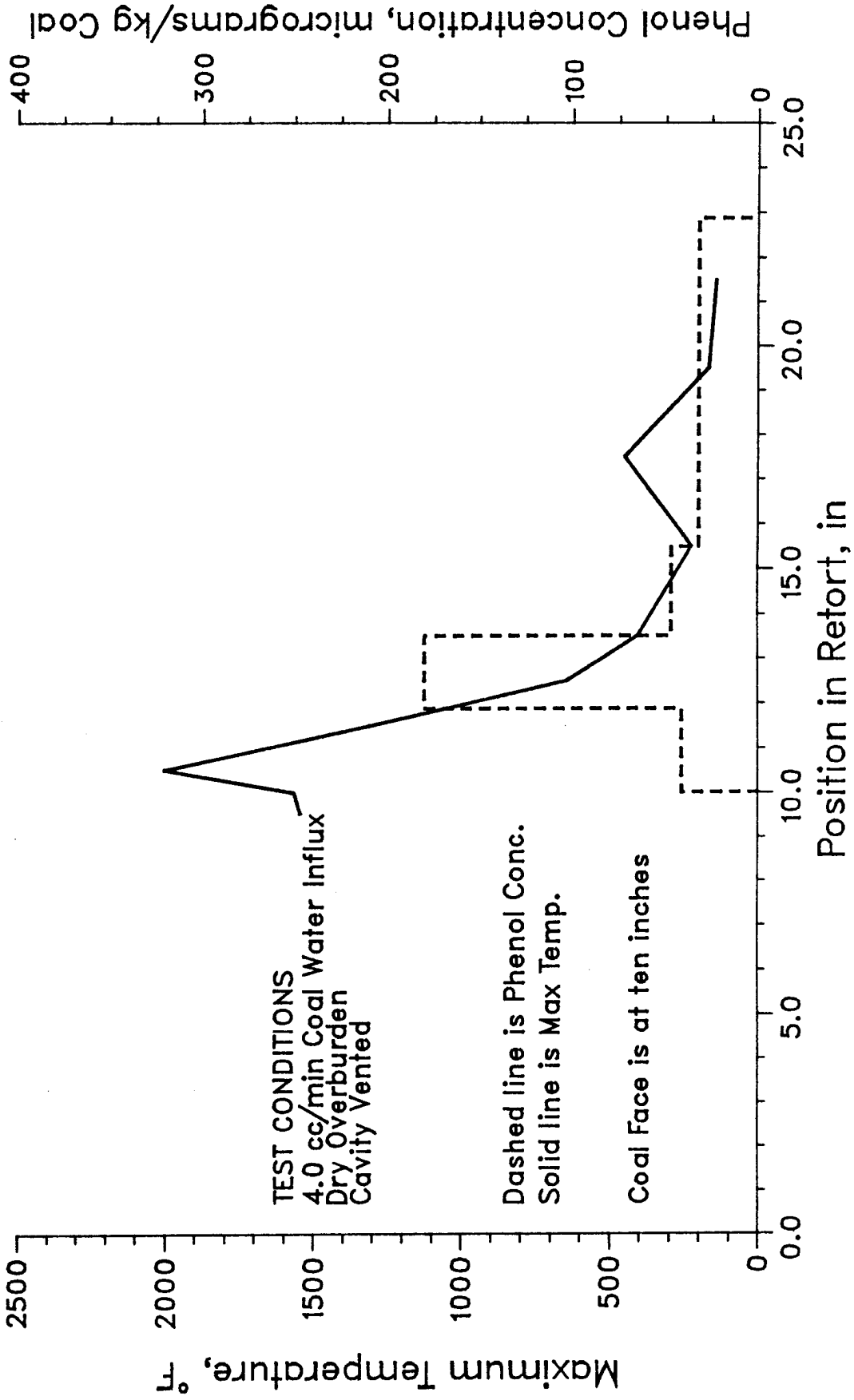


Figure D-2. Maximum Temperature and Phenol Concentration Versus Position for Experiment No. 6

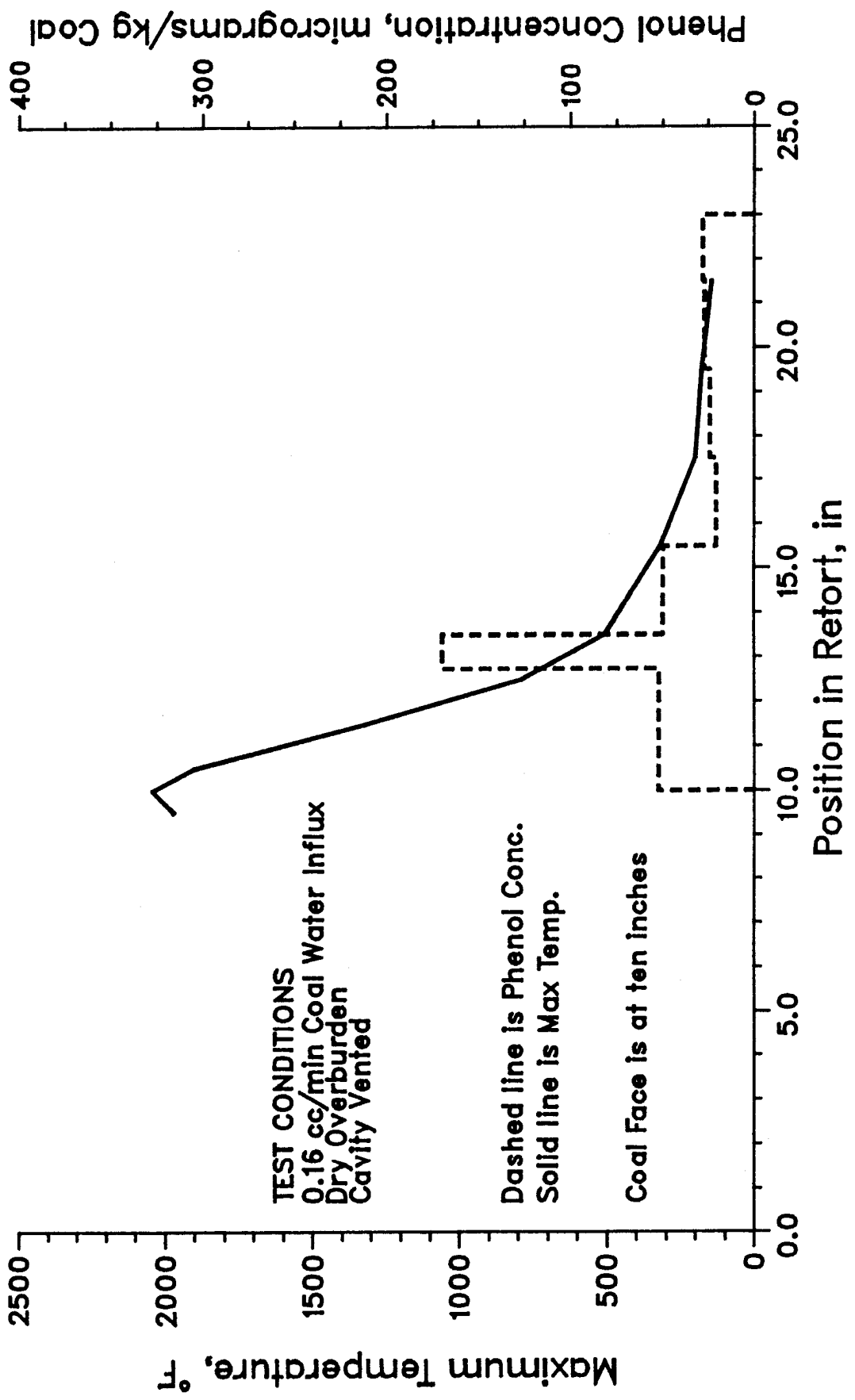


Figure D-3. Maximum Temperature and Phenol Concentration Versus Position for Experiment No. 7

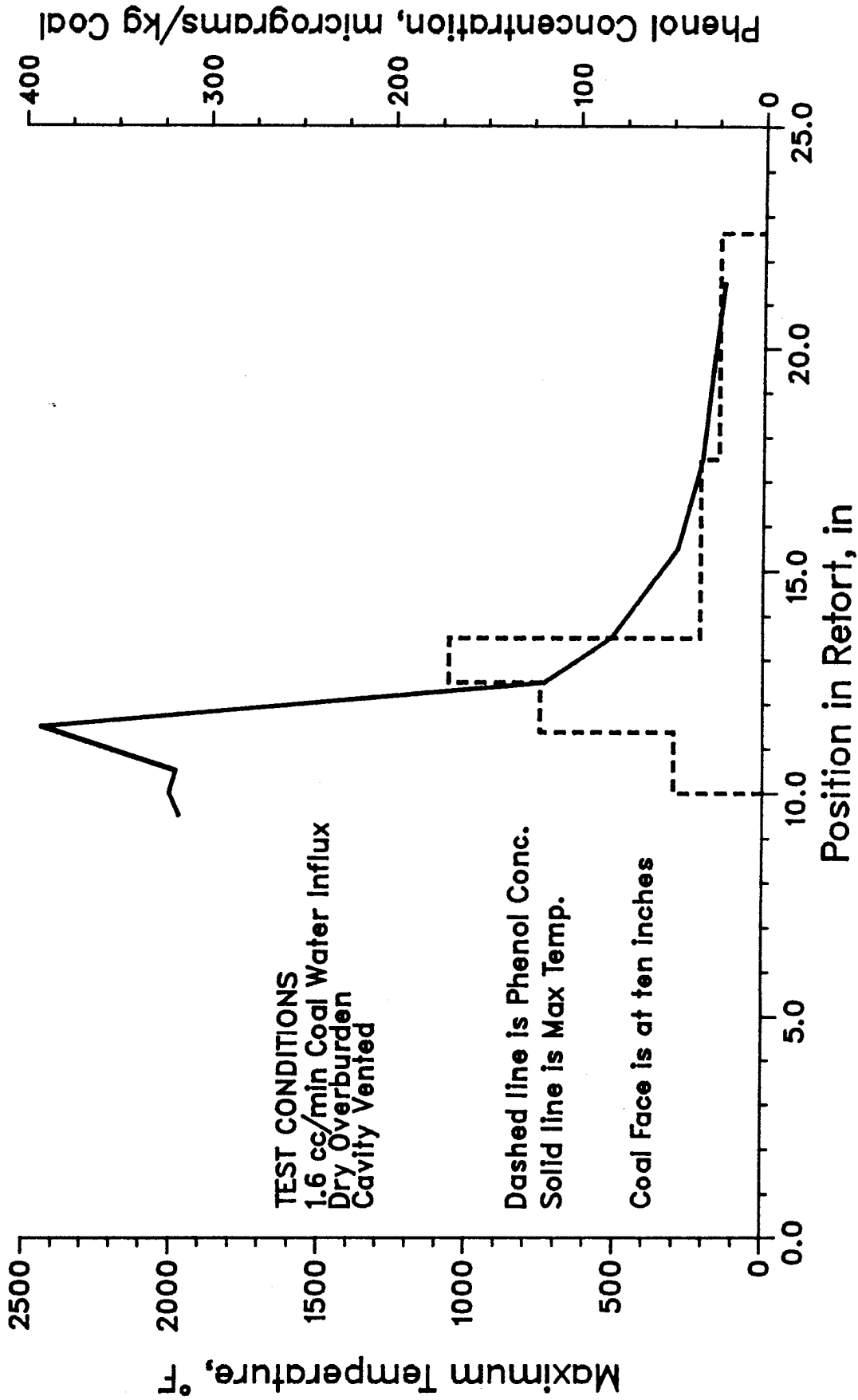


Figure D-4. Maximum Temperature and Phenol Concentration Versus Position for Experiment No. 8

APPENDIX E. EXPERIMENTAL DATA FOR OTHER EXPERIMENTS

Table E-1. Total Organic Carbon (TOC) Concentrations

Experiment #	Injected Water (mg/L)	Produced Liquid (mg/L)
3	<10 ^a	950
4	"	N.D. ^b
5	"	760
6	"	190, 35, 20, 20, 30 (50)
7	"	2400
8	"	460, 210, 85

^a Value less than the detection limit for the analytical procedure.
^b No data (sample container broken).

Table E-2. Sulfate Concentrations

Experiment #	Injected Water (mg/L)	Produced Liquid (mg/L)
3	27	<100
4	26	N.D. ^a
5	26	75
6	27	79, 27, 49, 45, 47, (63)
7	27	<290
8	28	330, 260, 230

^a No data (sample container broken).

Table E-3. Ammonia (NH₃-N) Concentrations^a

Experiment #	Injected Water (mg/L)	Produced Liquid (mg/L)
3	<10 ^b	230
4	"	N.D. ^c
5	"	98
6	"	33, 3.5, 3.0, 2.3, 2.8 (9.0)
7	"	810
8	"	240, 97, 20

^a Presented as the concentration of nitrogen in the ammonia.

^b Value less than the detection limit for the analytical procedure.

^c No data (sample container broken).

Table E-4. Boron (B) Concentrations

Experiment #	Injected Water (mg/L)	Produced Liquid (mg/L)
3	0.014	<.02
4	<.01 ^a	N.D. ^b
5	"	<.02
6	"	0.041, <0.1 ^c , (<.02)
7	"	0.110
8	"	0.372, 0.353, <0.1 ^a

^a Value less than the detection limit for the analytical procedure.

^b No data (sample container broken).

^c This concentration was found in four of the five samples from Experiment 6.

Table E-5. Fluoride (F) Concentrations

Experiment #	Injected Water (mg/L)	Produced Liquid (mg/L)
3	0.3	8
4	0.2	N.D. ^a
5	0.2	12
6	0.2	2
7	0.2	12
8	0.2	7

^a No data (sample container broken).

Table E-6. Barium (Ba) Concentrations

Experiment #	Injected Water (mg/L)	Produced Liquid (mg/L)
3	0.074	.109
4	0.078	N.D. ^a
5	0.078	.140
6	0.077	.129
7	0.079	.072
8	0.078	.050

^a No data (sample container broken).

Table E-7. Arsenic (As) Concentrations

Experiment #	Injected Water ($\mu\text{g/L}$)	Produced Liquid ($\mu\text{g/L}$)
3	<5 ^a	14
4	"	N.D. ^b
5	"	15
6	"	10
7	"	<15
8	"	21

^a Value less than the detection limit for the analytical procedure.

^b No data (sample container broken).

Table E-8. Selenium (Se) Concentrations

Experiment #	Injected Water ($\mu\text{g/L}$)	Produced Liquid ($\mu\text{g/L}$)
3	<5 ^a	<10
4	"	N.D. ^b
5	"	<13
6	"	<5
7	"	95
8	"	<15

^a Value less than the detection limit for the analytical procedure.

^b No data (sample container broken).

Table E-9. Lead (Pb) Concentrations

Experiment #	Injected Water ($\mu\text{g/L}$)	Produced Liquid ($\mu\text{g/L}$)
3	<2 ^a	71
4	16	N.D. ^b
5	<2 ^a	60
6	2	62
7	<2 ^a	60
8	<2 ^a	24

^a Value less than the detection limit for the analytical procedure.

^b No data (sample container broken).

Table E-10. Mass of Contaminant Species In the Produced Liquids^a

Experiment #	Mass of Sample (grams)	TOC (mg)	SO ₄ (mg)	NH ₃ -N ^b (mg)	F (mg)	B (µg)	Ba (µg)	As (µg)	Se (µg)	Pb (µg)
3	376.3	357	<38 (<34)	87	3	<8 (<6)	41 (30)	5	<4	27
5	369.0	280	28 (5)	36	4	7	52 (-18)	6	<5	22
6	384.4 501.1 472.2 466.3 <u>282.9</u> 2,106.9	73 18 9 9 <u>6</u> 115	30 14 23 21 <u>16</u> 104 (88)	13 2 1 1 <u>1</u> 18						
					4	16	272 (226)	21	<11	131
7	55.4	133	16 (11)	45	1	6	4 (-11)	<1	5	3
8	183.1 131.4 <u>433.3</u> 747.8	84 28 <u>37</u> 149	60 34 <u>100</u> 194 (134)	44 13 <u>9</u> 66		68 46 <u>0</u> 114				
					2		16 (-152)	7	<5	8

^a Values in parentheses indicate the net mass increase in the species (mass species in produced liquids collected - mass species in injected water) if significant contaminant is present in injected water.

^b Values reported for ammonia represent the mass of nitrogen in the ammonia.

Note: No data for experiment 4 (sample container broken).

Table E-11. Other Contaminant Species Generated During Coal Pyrolysis

Experiment #	TOC (mg/kg)	SO ₄ (mg/kg)	NH ₃ -N ^b (mg/kg)	B (µg/kg)	F (mg/kg)	Ba (µg/kg)	AS (µg/kg)	Se (µg/kg)	Pb (µg/kg)	Mass of Species in Produced Liquids ^a	
										Mass of Coal Pyrolyzed	
3	4650	<500 (<440)	1130	100 (80)	40	530 (390)	70	<50	350		
5	3275	330 (60)	420	80	50	610 (0)	70	<60	260		
6	3780	3420 (2890)	590	530	130	8940 (7430)	690	<360	4300		
7	2960	360 (250)	1000	130	20	90 (0)	<20	110	70		
8	3670	4780 (3300)	1630	2810	50	390 (0)	170	120	200		

^a Values in parentheses indicate the net mass increase in the species (mass species in produced liquids collected - mass species in injected water) if significant contaminant is present in the injected water.

^b Values reported for ammonia represent the mass of nitrogen in the ammonia.

Note: No data for experiment 4 (sample container broken).

